Biomineralization, biomimetic and non-classical crystallization

Ways to understand the synthesis and formation mechanisms of complex materials

Helmut Cölfen

Max-Planck-Institute of Colloids & Interfaces, Colloid Chemistry, Research Campus Golm, D-14424 Potsdam
Coelfen@mpikg-golm.mpg.de

$CaCO_3$ Biominerals

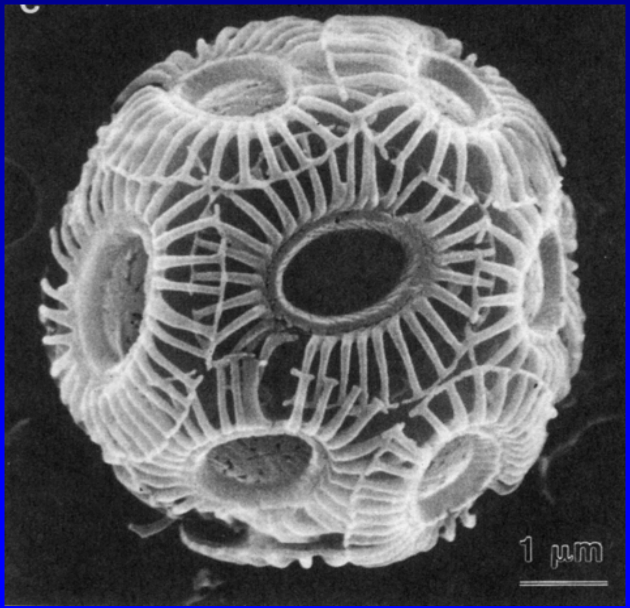

Coccolith (Calcite)

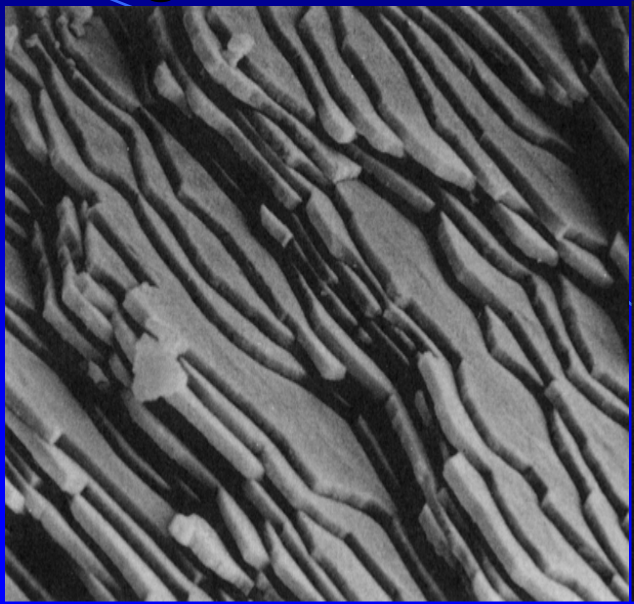

Nacre (Aragonite)

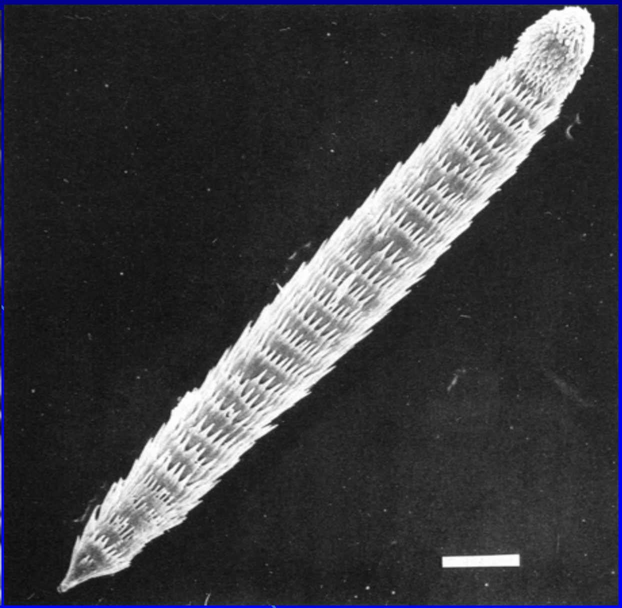

Herdmania momus (Vaterite)

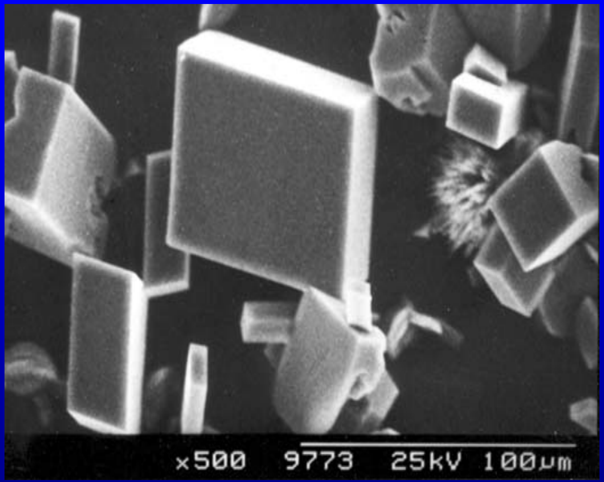

Default: Rhombohedral Calcite

Characteristics of Biominerals:
Complex forms generated from inorganic systems with simple structure

Characteristics of inorganic crystals:
Simple geometrical form but often complicated crystal structure

Important biominerals

Mineral	Formula	Function
Calciumcarbonate	$CaCO_3$	
Calcite		Algae / Exoskeleton
		Birds / Eggshell
Aragonite		Fishes / Gravity sensor
		Mussels / Exoskeleton
Vaterite		Sea urchins / Spikes
Calciumphosphate		
Hydroxyapatite	$Ca_{10}(PO_4)_6(OH)_2$	Vertebrates / Skeleton, teeth
Octa-Calciumphosphate	$Ca_8H_2(PO_4)_6$	Vertebrates / Precursor for bone formation
Silica	SiO_2	Algae / Exoskeleton
Iron oxide		
Magnetite	Fe_3O_4	Salmon, Tuna & bacteria / Magnetic field sensor
		Chitons / teeth

Evolution of a mussel shell

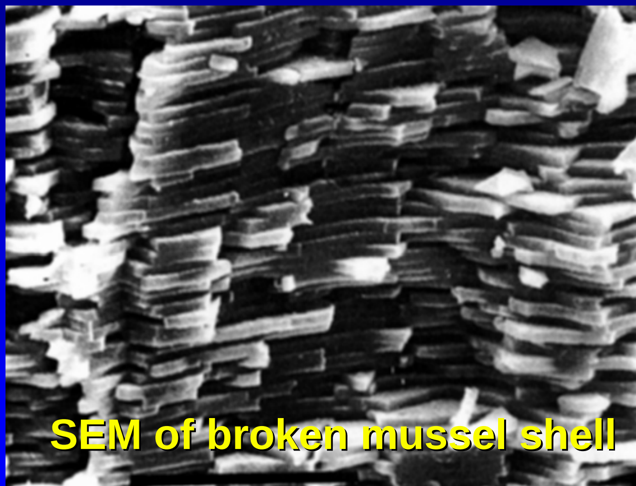

SEM of broken mussel shell

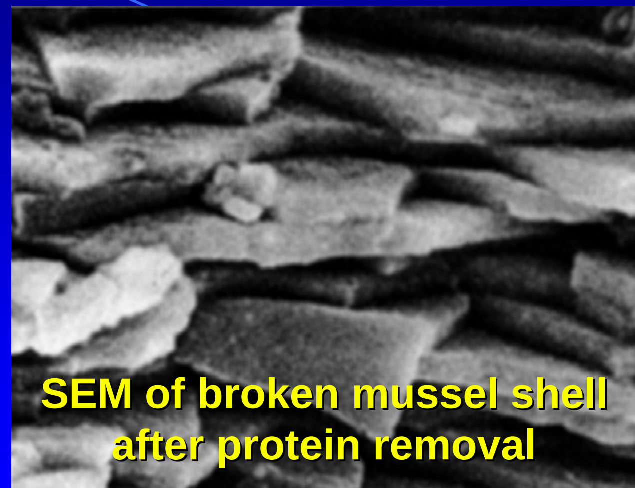

SEM of broken mussel shell after protein removal

SEM of broken mussel shell after $CaCO_3$ removal

TEM thin cut of developing mussel shell

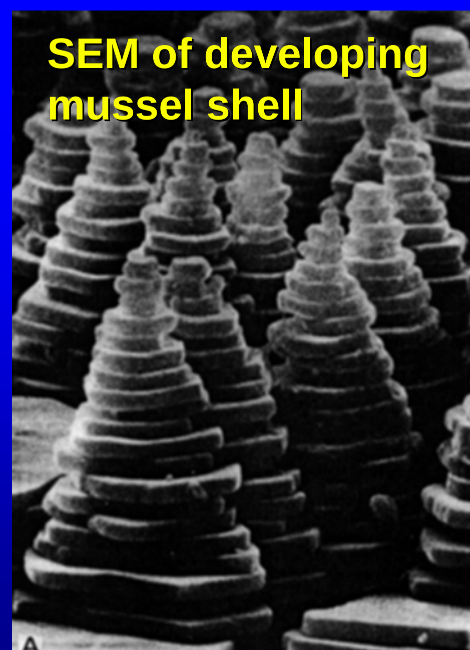

SEM of developing mussel shell

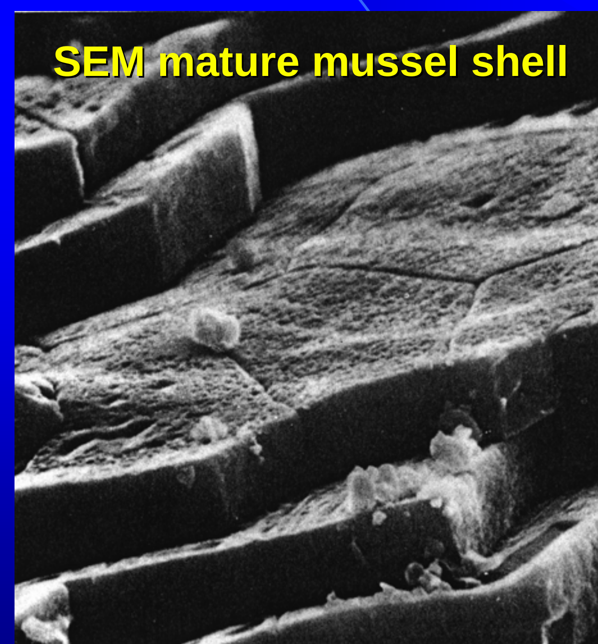

SEM mature mussel shell

Biominerals are often formed in confined reaction environments

Epitactical match between crystal and matrix

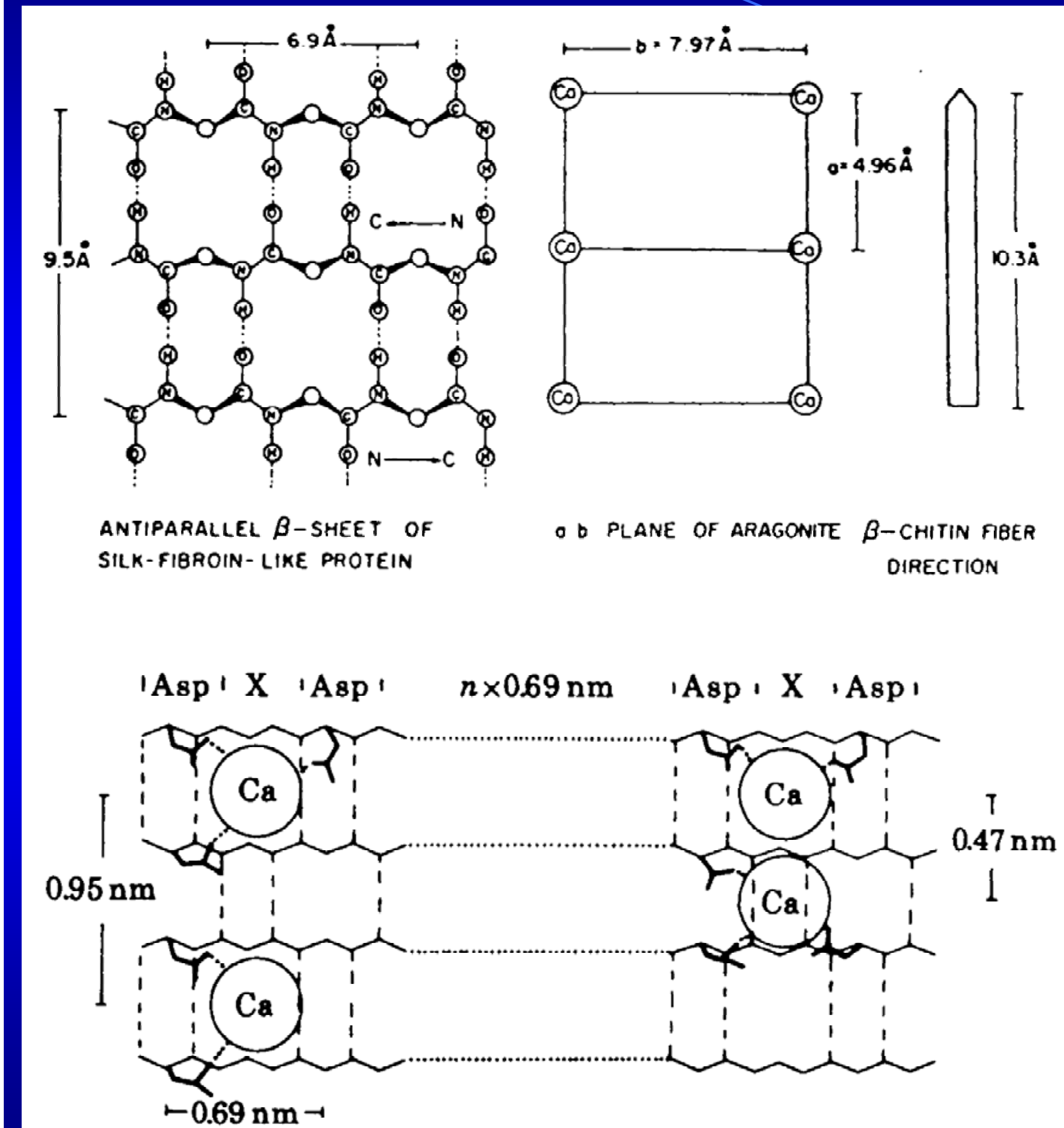

Nacre:

Periodicity in protein β-sheets and β-chitin fibers in close geo-metrical match to lattice spacing of aragonite 001 face.

„Soft Epitaxy“

Bone formation

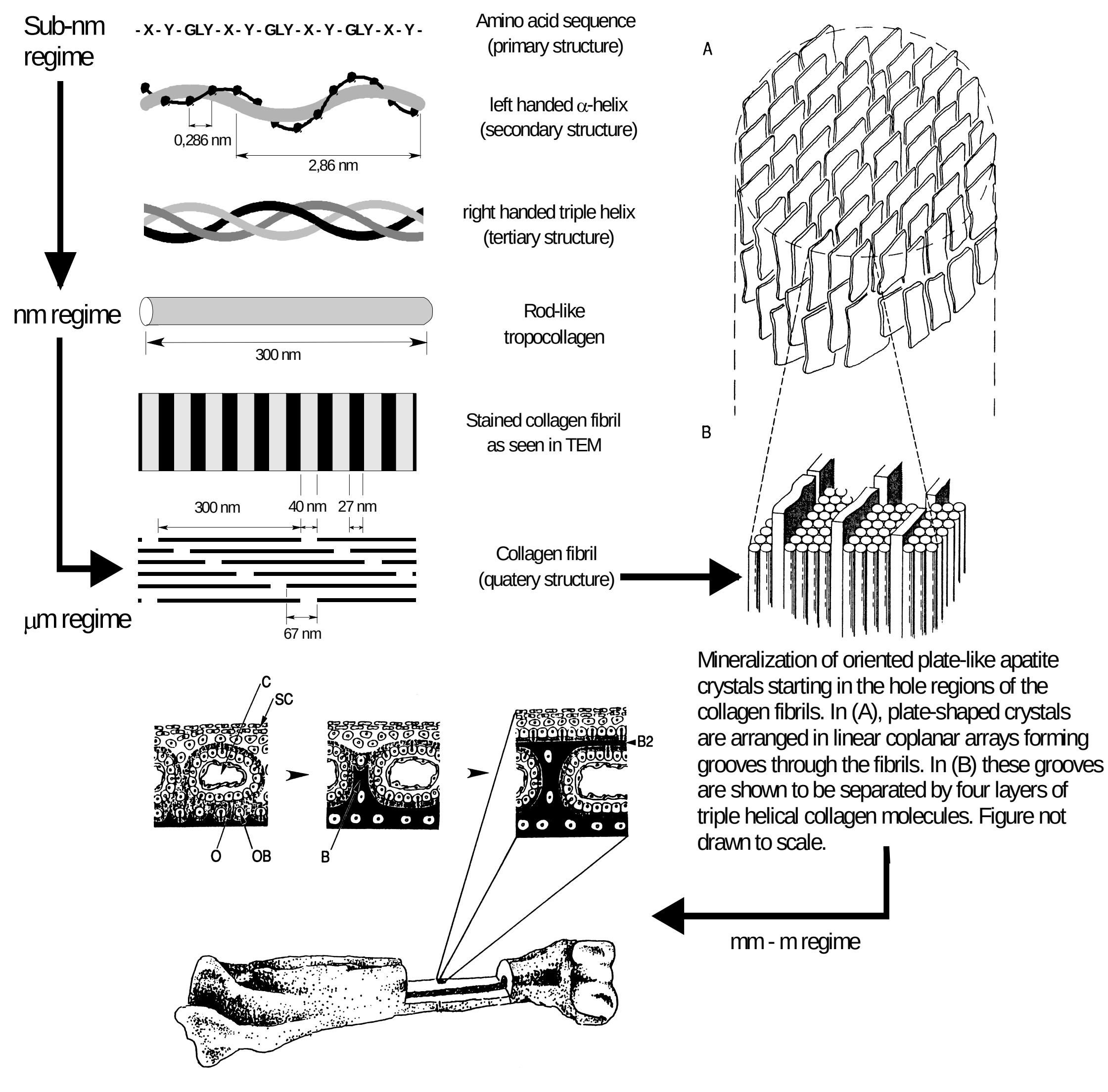

Sequence of progressive bone development. Osteoblasts (OB) oriented with their backs toward the capillary vasculature (C), secrete osteoid (O) away from the vasculature, causing the formation of a bony strut (B), and eventually forming a second layer of bone (B2). The stacked layer (SC), which provides osteoprogenitor cells for the process, continues to expand in the direction of bone growth.

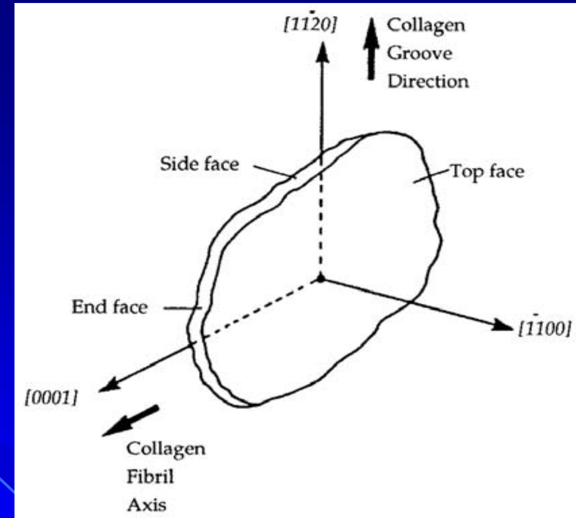

Characteristics:

Mineralization occurs in organic matrix

Superstructure formation over several length scales

Here over 9 magnitudes in length !
From almost atomic to macroscopic scale

Tooth enamel

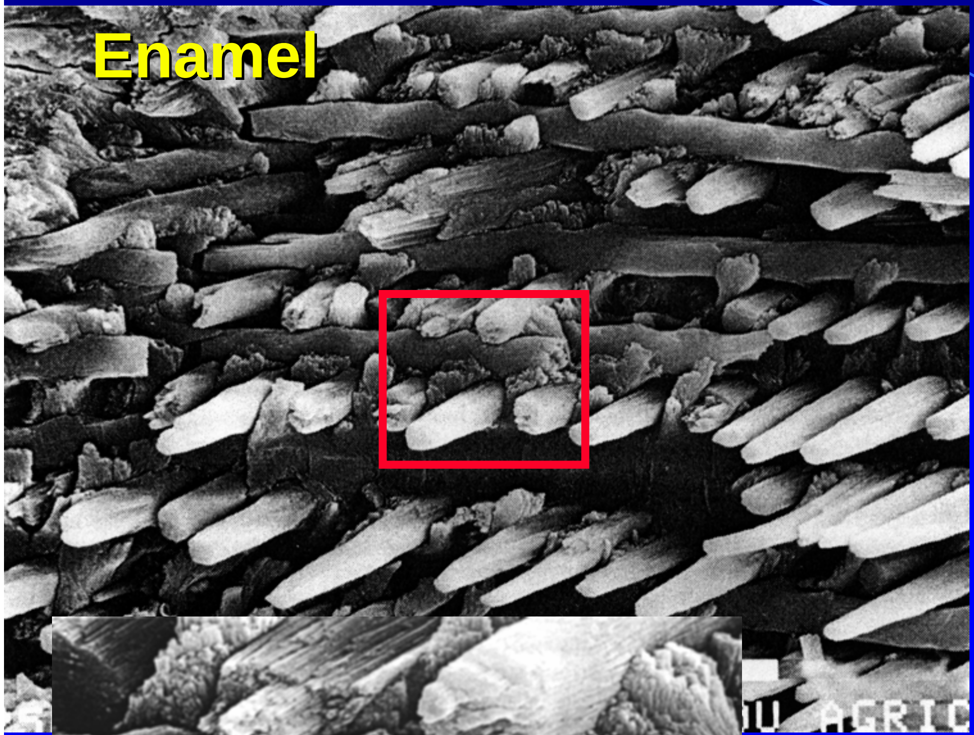

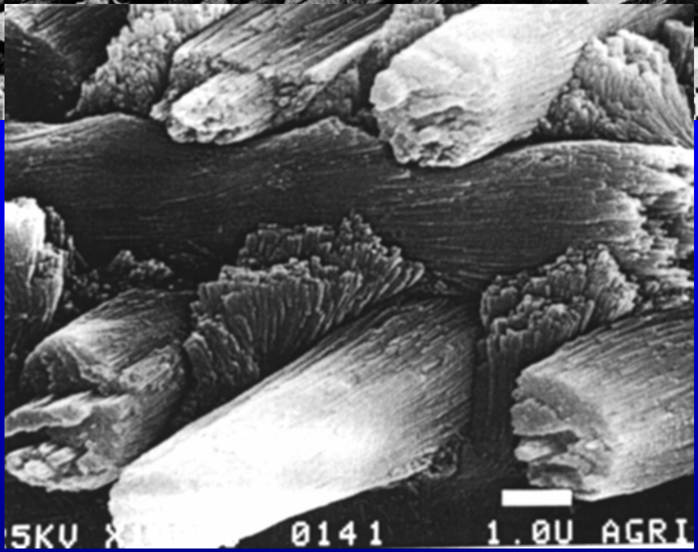

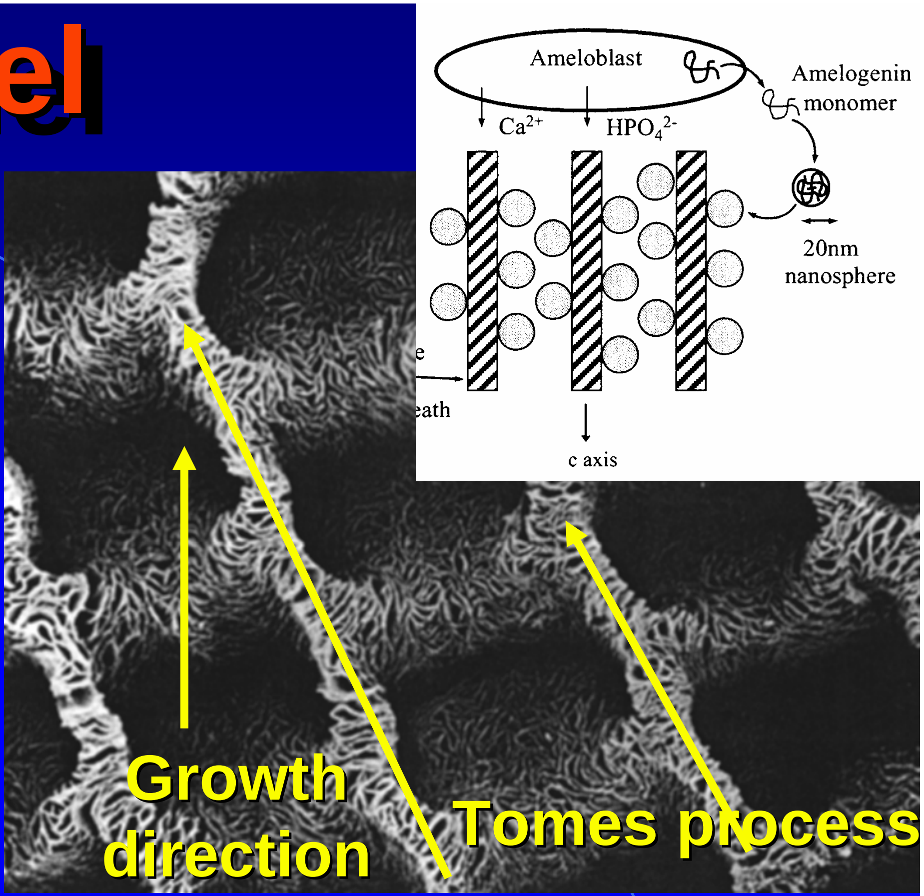

- Crystallization and assembly of fibers into rods on the μm scale
- Ordered layer structure of rods provides mechanical strength
- Permanent further crystallization and density increase up to 95 wt.-% mineral

Crystallization often occurs highly directed

Magnetotactic bacteria

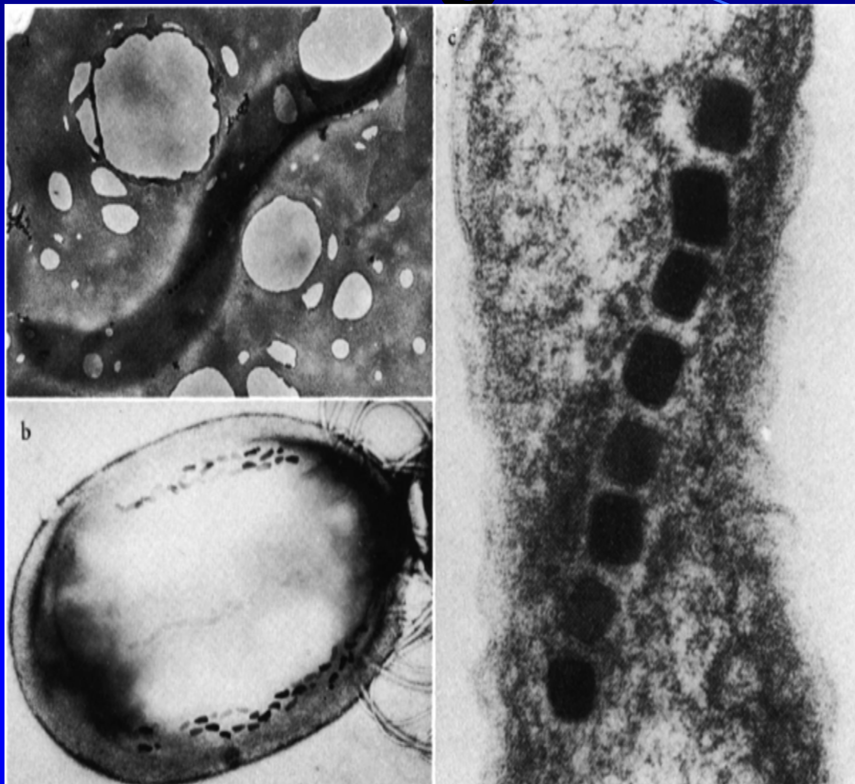

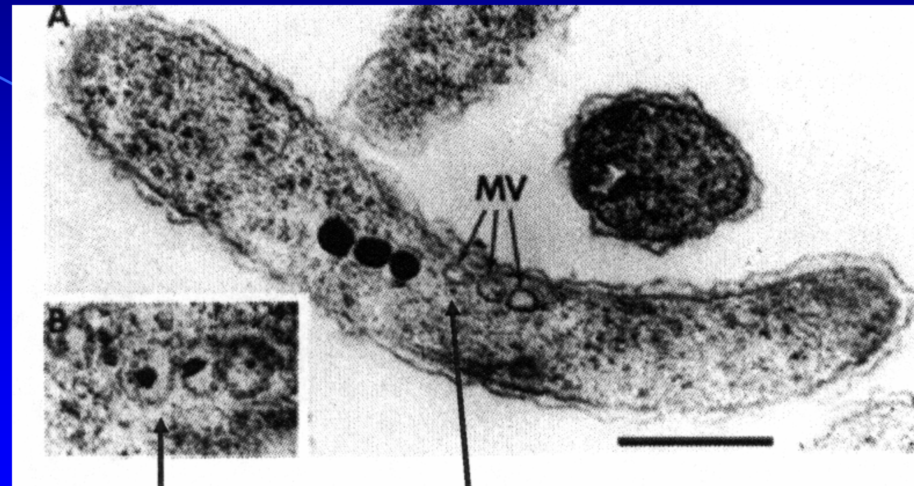

Nucleation on inside wall of vesicle

Linear organization for magnetic compass

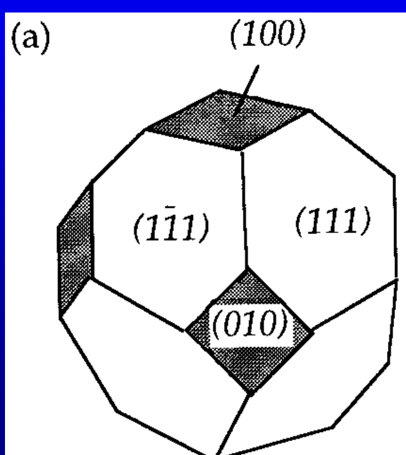

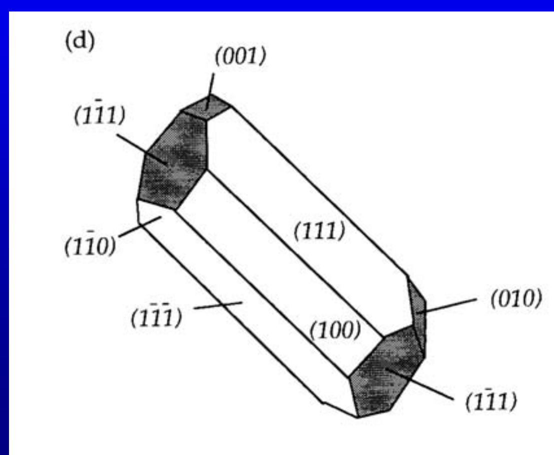

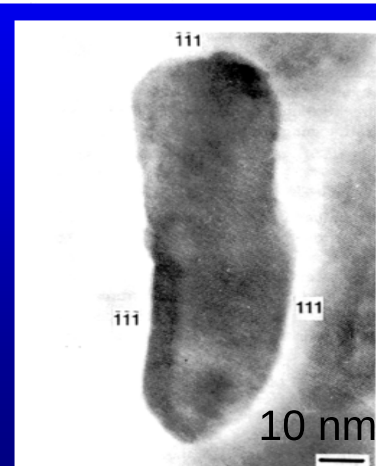

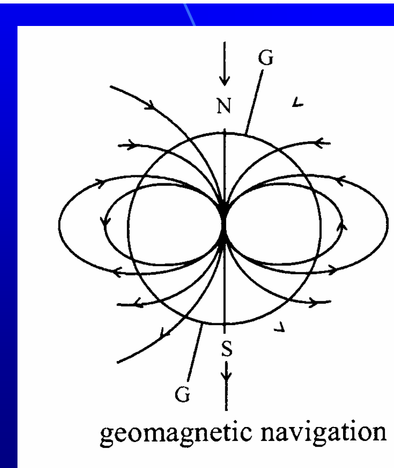

Phase transitions and matrix assisted nucleation

Adapted from S.Mann IMPRS lectures, Golm 2003

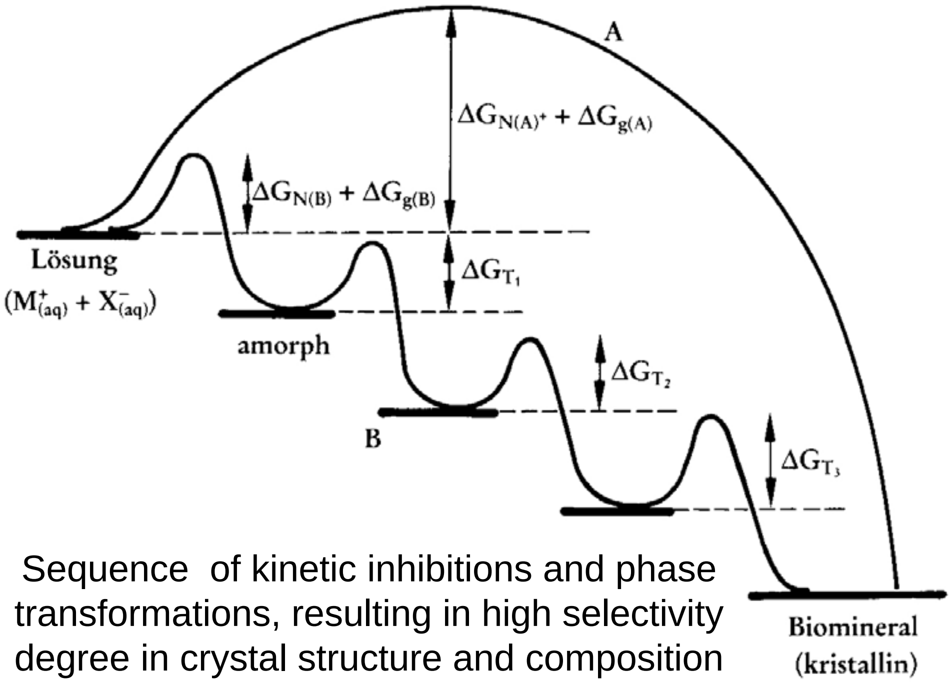

Sequence of kinetic inhibitions and phase transformations, resulting in high selectivity degree in crystal structure and composition

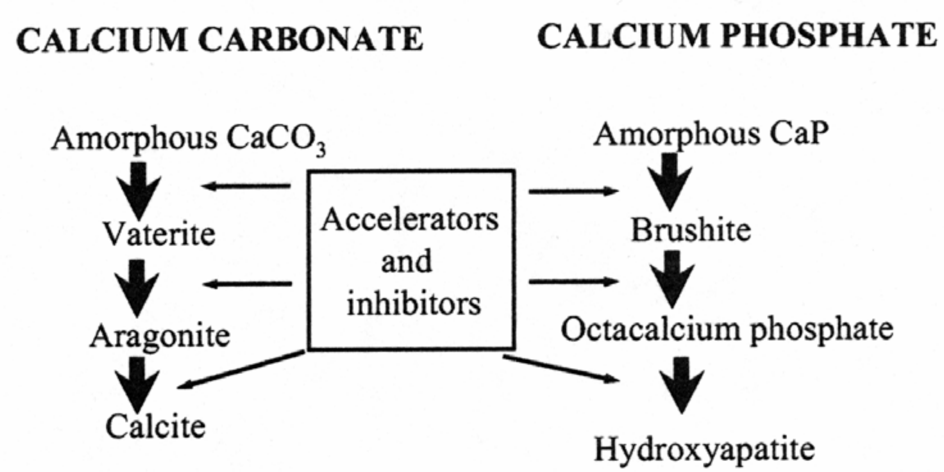

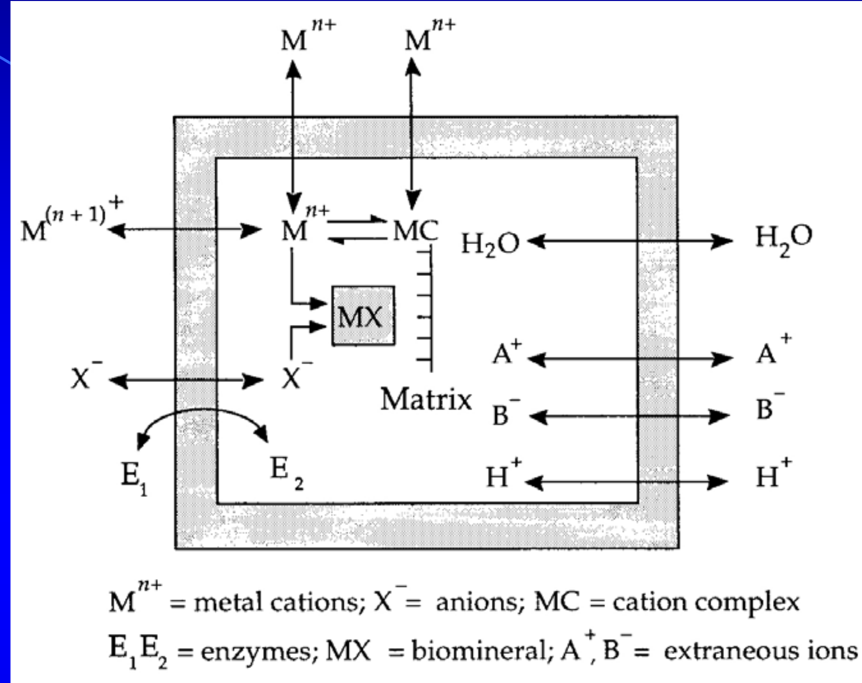

Direct mechanisms to increase S:

Ion pumping + redox

Ion complexation/decomplexation

Enzymatic regulation

Indirect mechanisms to increase S:

Ion transport

Water extrusion

Proton pumping

General biomineralization features

- Uniform particle size
- Well defined structure and composition
- High levels of spatial organization
- Complex morphologies
- Controlled aggregation and texture
- Preferential crystallographic orientation
- Higher order assembly
- Hierarchical structures

Adapted from S.Mann IMPRS lectures, Golm 2003

Known mechanisms of Biomineralization

- Stabilization
- Morphology control by selective adsorption
- Control of the crystal modification by „Soft Epitaxy“
- Static templates
- Confined reaction environments
- Adaptive construction and synergistic effects
- Structural reconstruction
- Higher order assembly

Polymer structures as static templates

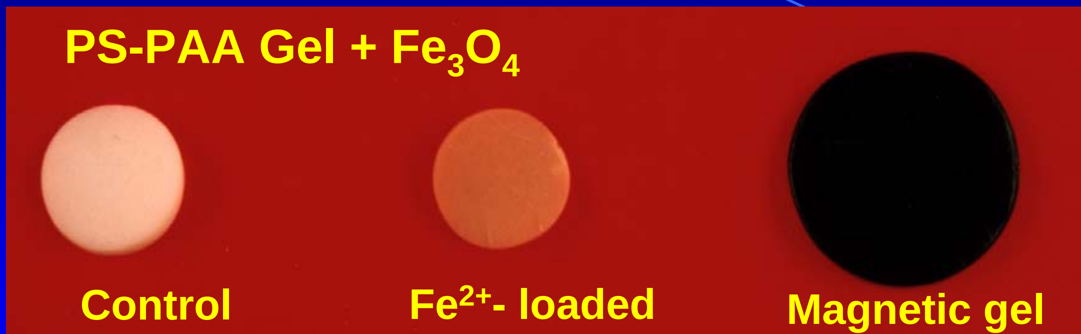

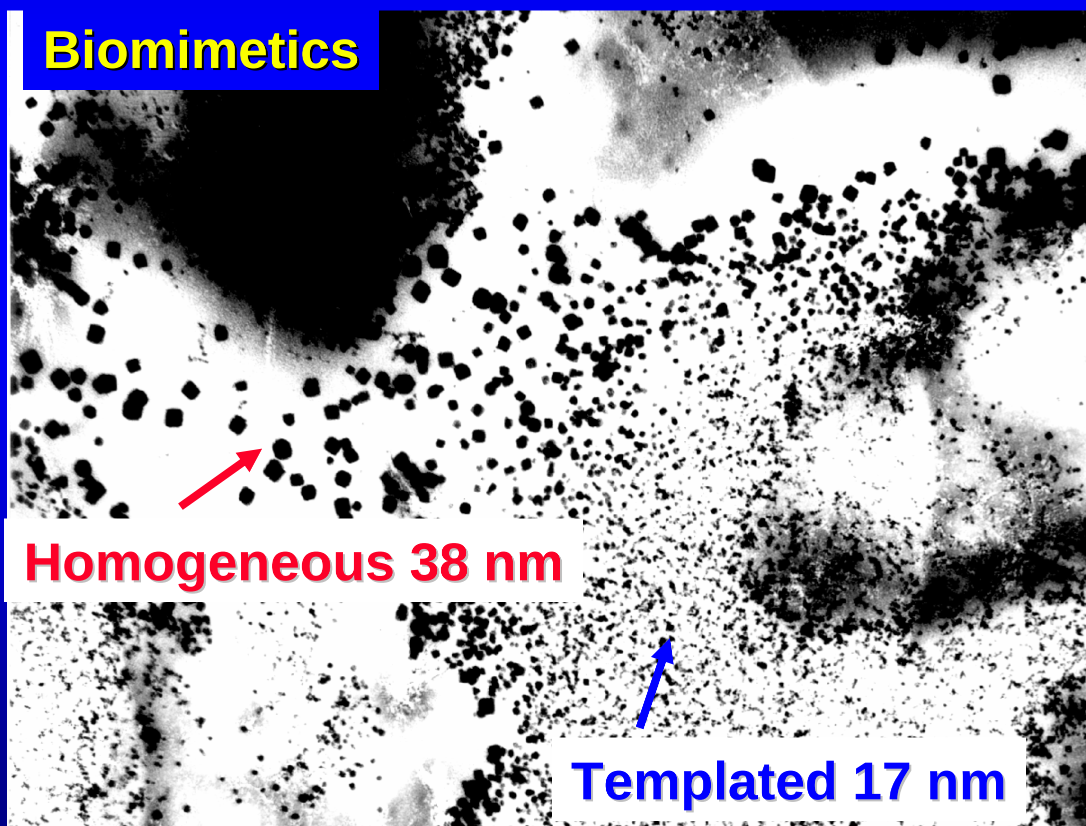

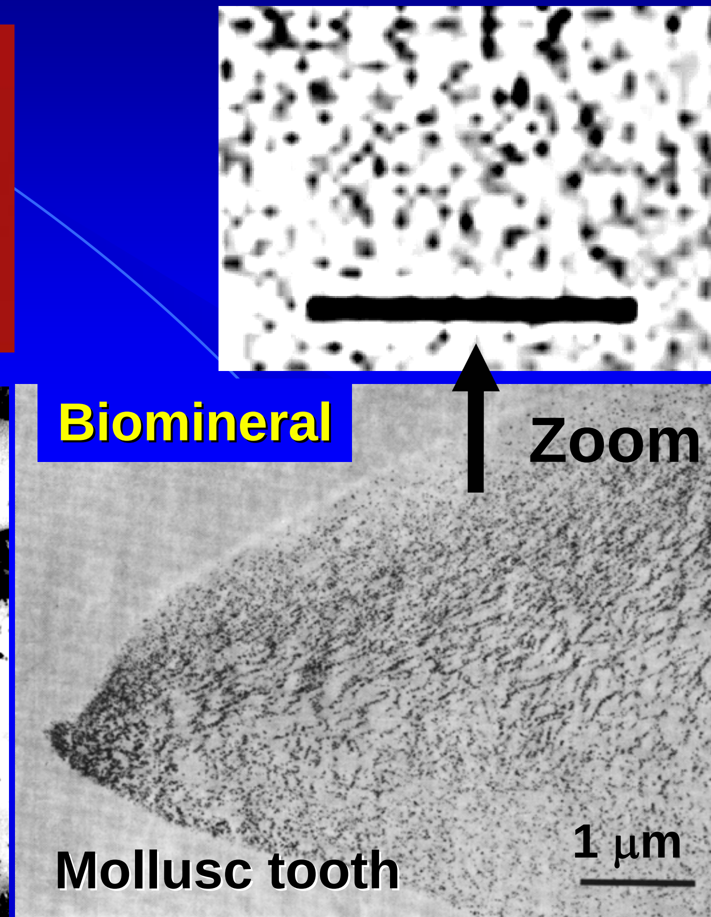

Fe_3O_4 15 - 35 nm
in Polysaccharide -
Protein Gel

M. Breulmann, H.P. Hentze

Double hydrophilic block copolymers

Molecular tool:

= hydrophilic, interacting with mineral

= hydrophilic, non interacting with mineral

Amphiphilic behaviour induced in presence of mineralic surfaces

allows - Size/shape control

- Stabilization

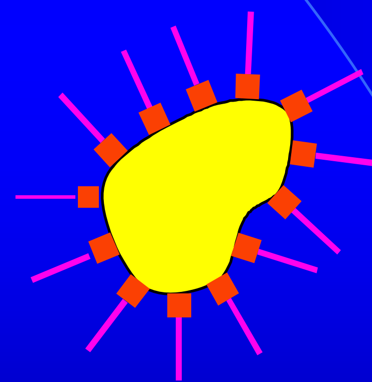

Advantage of DHBC design for $CaCO_3$

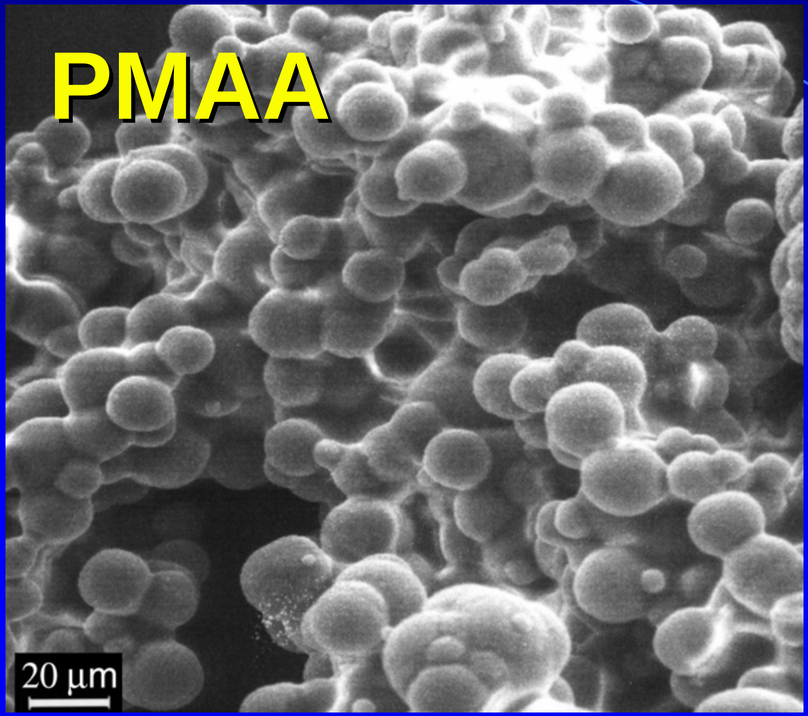

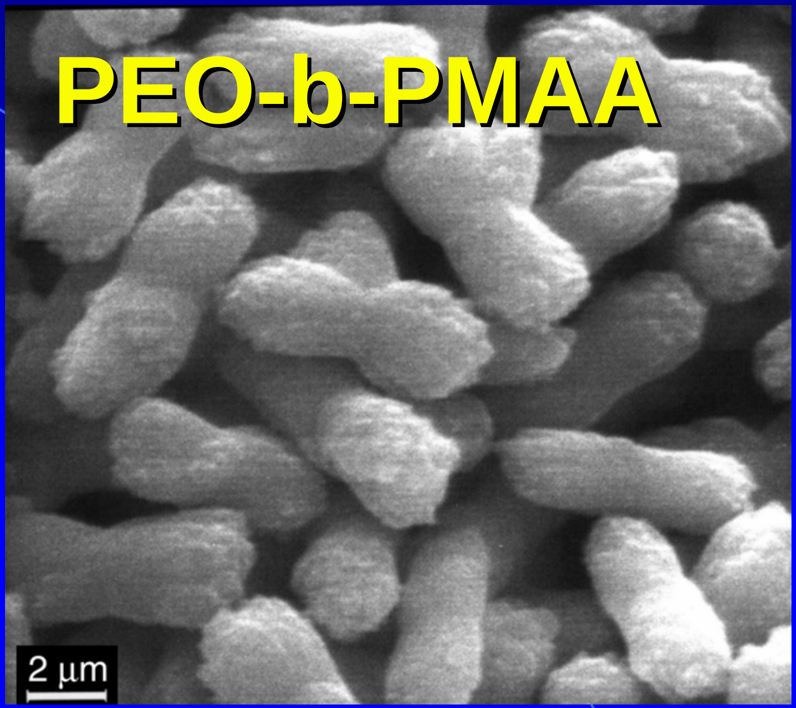

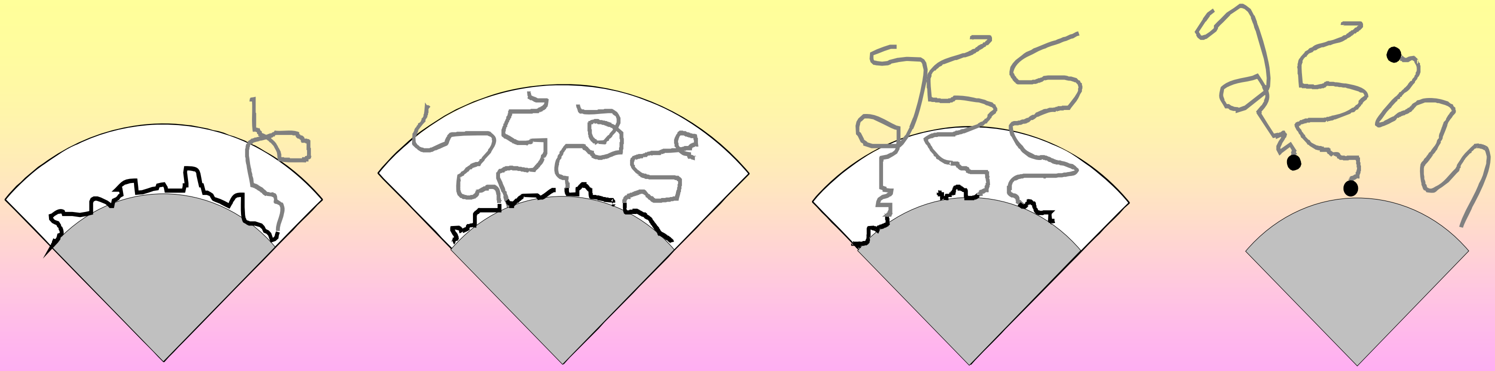

PE block too long, stab. block too short

PE block and stab. block good ratio

PE block too short, stab. block too long

PE block far too short, stab. block too long

Double hydrophilic block copolymers

Precursor Polymers

PEG-*b*-PEI

(Linear and branched)

PEG-*b*-PMAA

PEG-*b*-PB

Modular Synthesis

M = 3000 – 10000 g/mol

Functionalities

OH **COOH**

SO_3H

PO_3H_2 **PO_4H_2**

CH_3SCN

NR_3, HNR_2, H_2NR

Hydrophobic

M. Sedlak, M. Breulmann, J. Rudloff, P. Kasparova, S. Wohlrab, T.X. Wang

$BaSO_4$ Morphogenesis at pH 5

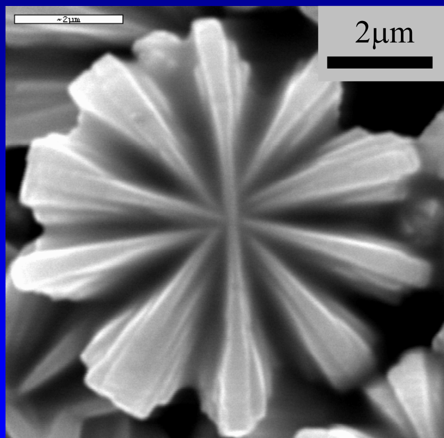

PEG-*b*-PEI-SO_3H

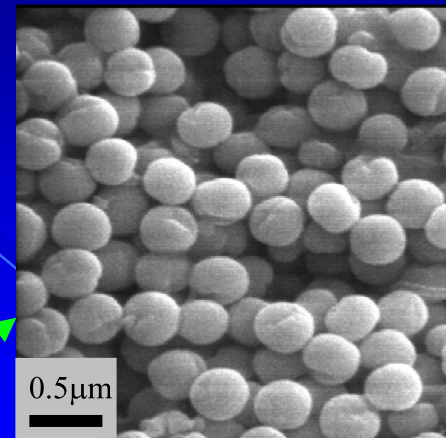

PEG-*b*-PMAA-Asp

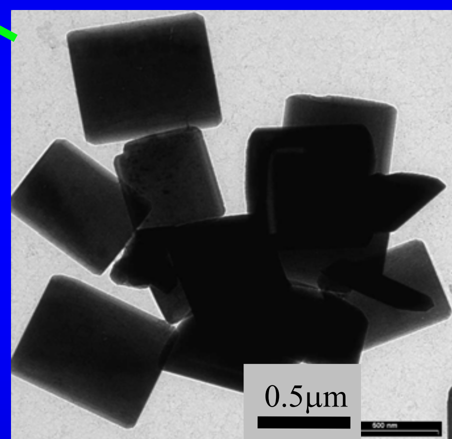

No additive

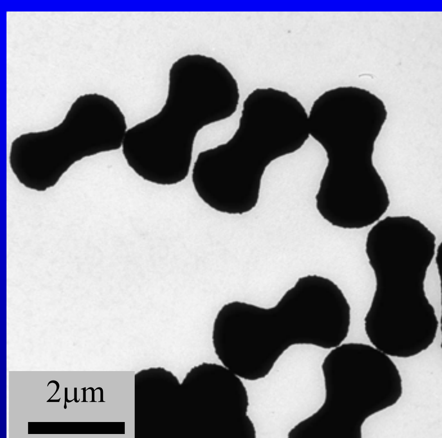

PEG-*b*-PEI-COOH

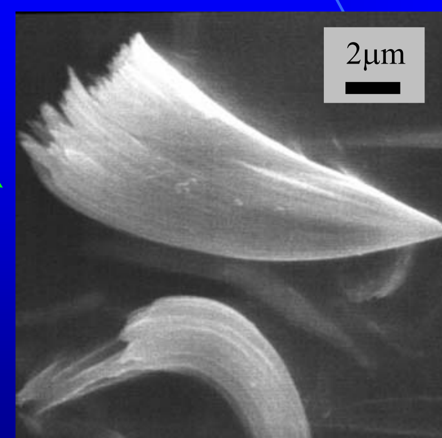

PEG-*b*-PMAA-PO_3H_2

L.M. Qi

CdS + PEO-*b*-PEI$_{branched}$

L.M. Qi

- Particle size adjustable 2 - 4 nm
- Monodisperse stable particles
- No photooxidation
- Branched PEI more effective than linear or dendrimer

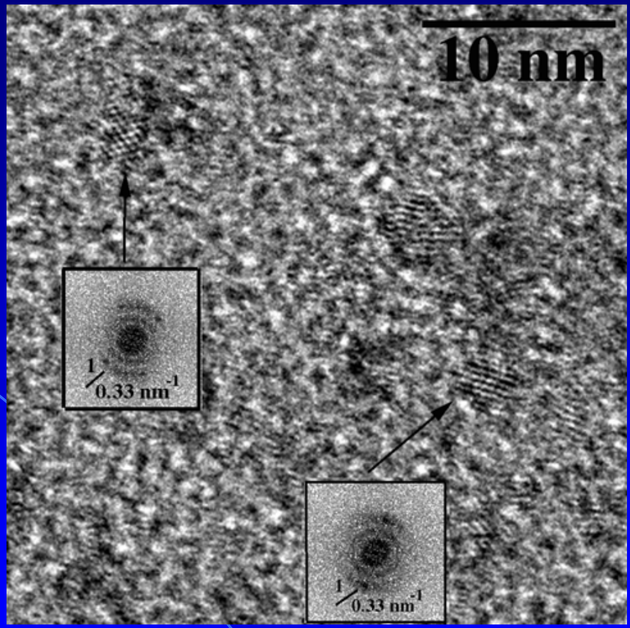

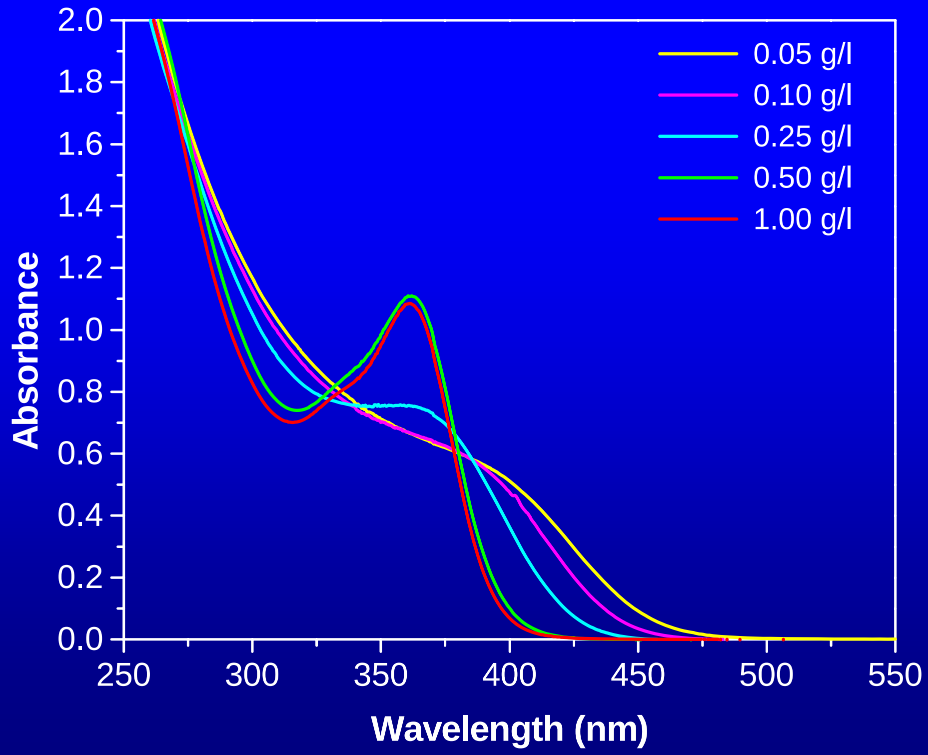

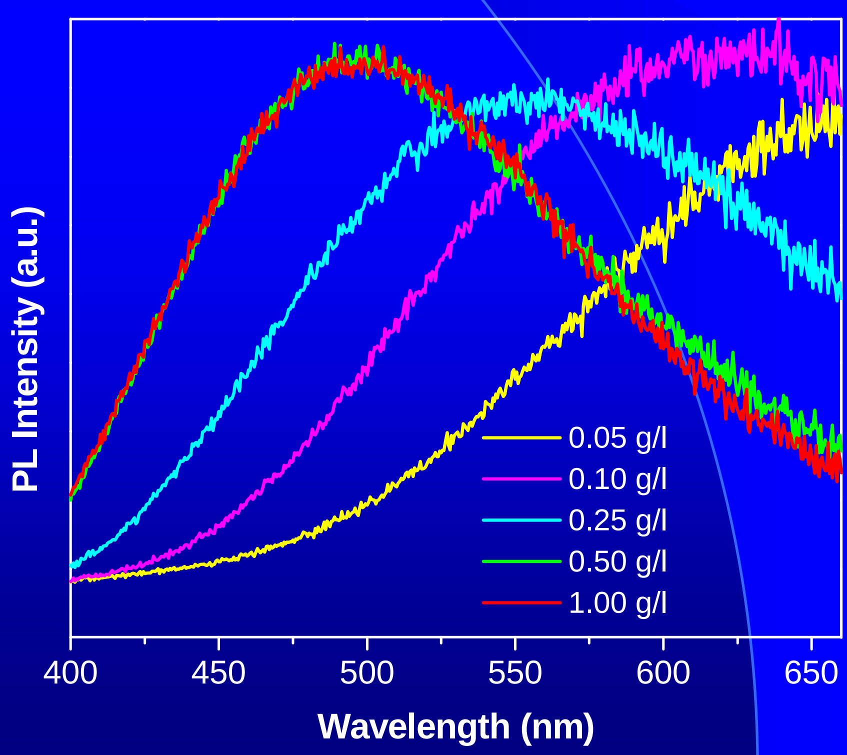

Selective Adsorption

Gold crystallized in presence of PEG-*b*-1,4,7,10,13,16-Hexaazacycloocatadecan (Hexacyclen) EI macrocycle

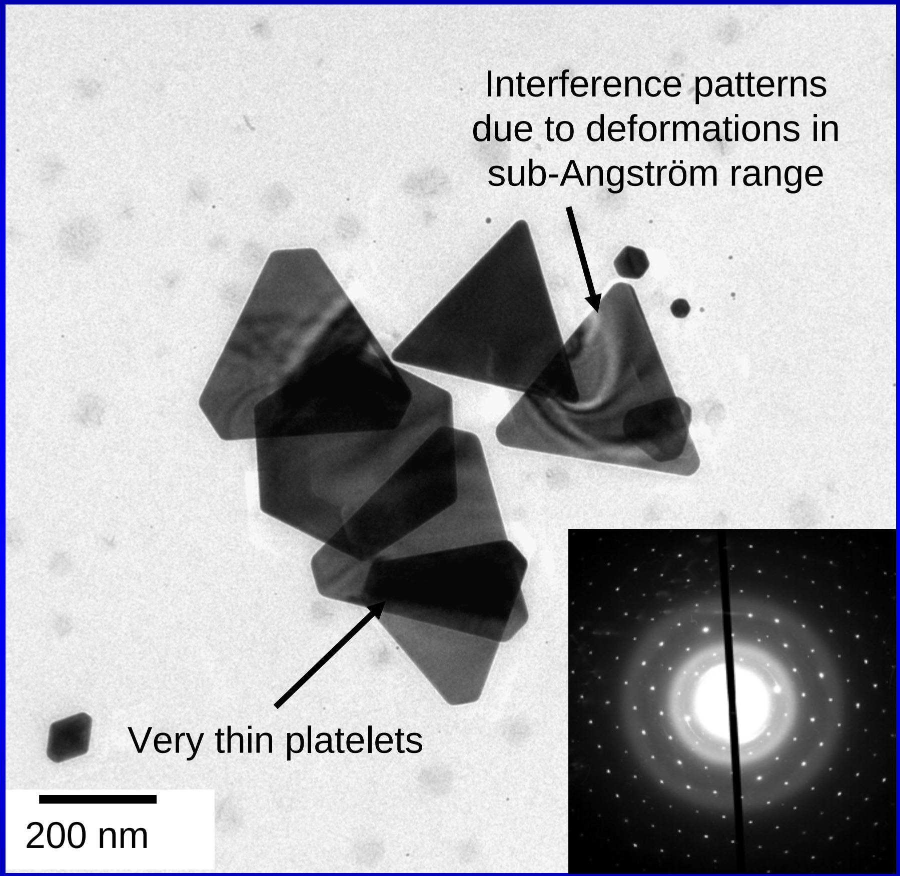

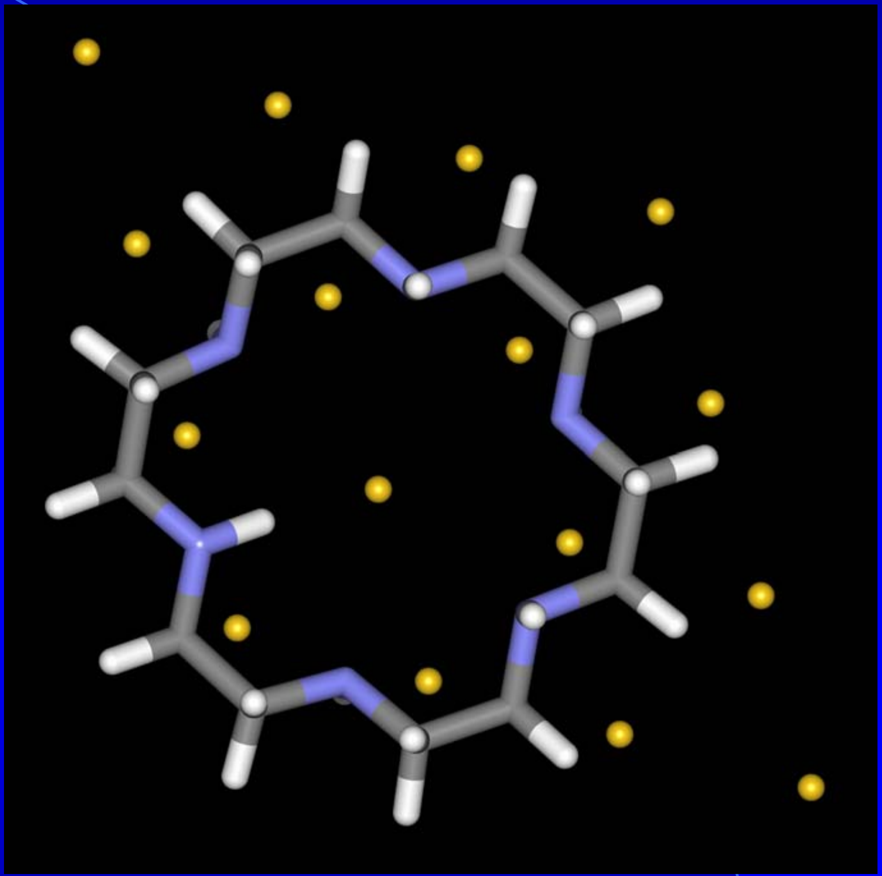

Very thin platelets with exposed 111 surface, Well developed plasmon band in UV/Vis

Au (111) surface and adsorbed hexacyclen molecule in vacuum

S.H. Yu

Surfaces as static template

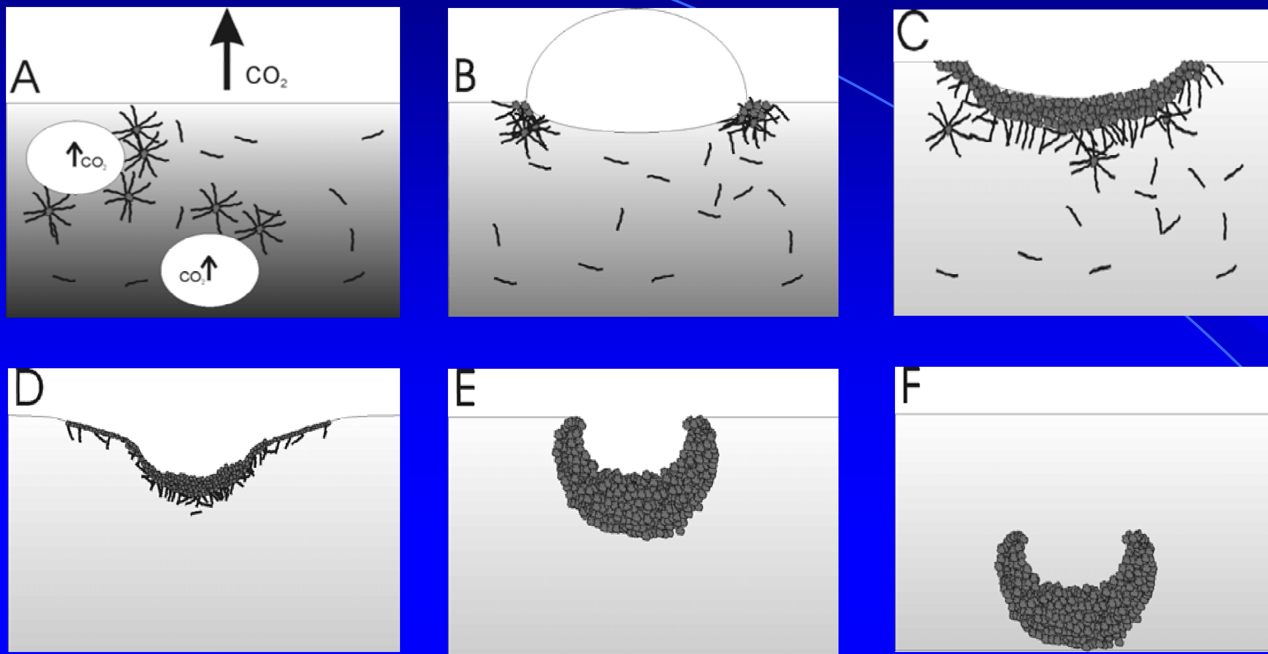

$CaCO_3$ +

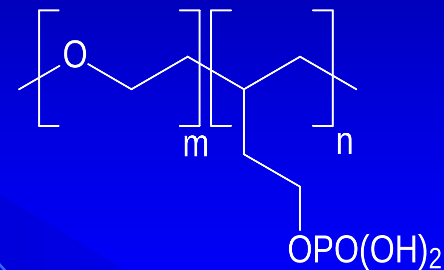

PEG(m)-*b*-PHEE(n)-($P_{G\ rad}$%)

J. Rudloff

$$CaCO_{3(s)} + CO_{2(g)} + H_2O_{(l)} \rightleftharpoons Ca^{2+}_{(aq)} + 2\ HCO_3^-{}_{(aq)}$$

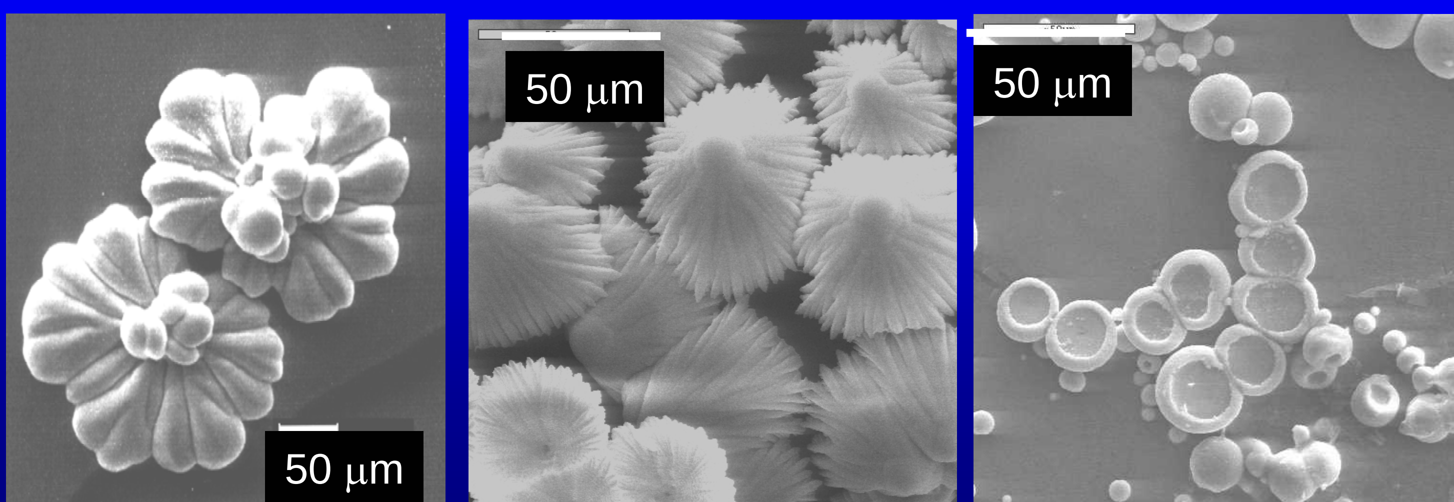

Structural reconstruction

pH = 5

$BaSO_4$ with PEG-*b*-PMAA-PO_3H_2

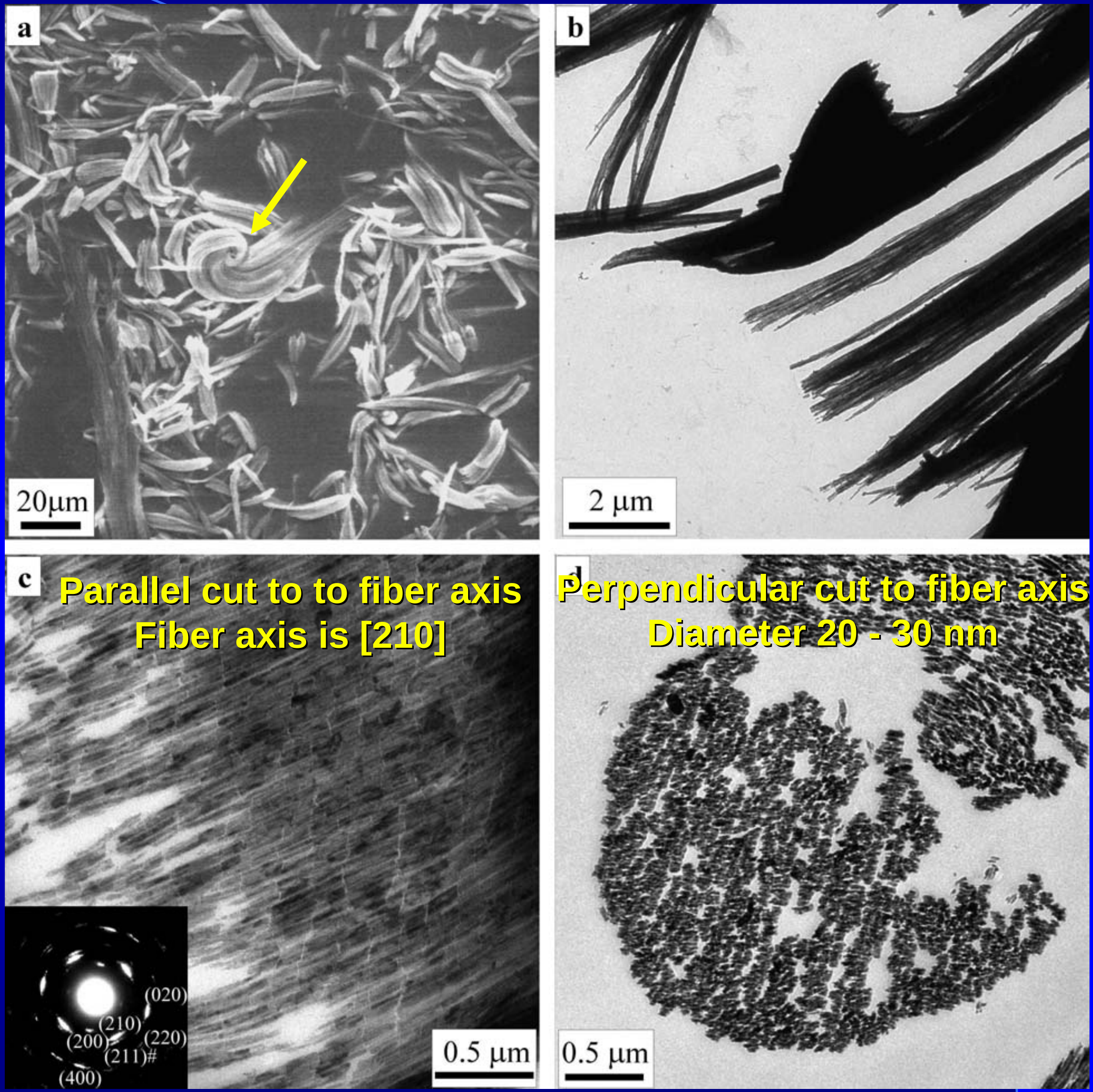

Bundles of single crystalline fibers

L.M. Qi

Structural reconstruction

pH = 5

$BaSO_4$ fibers obtained in the presence of PEG-*b*-PMAA-PO_3H_2 on carbon films with an aging time of 5d.

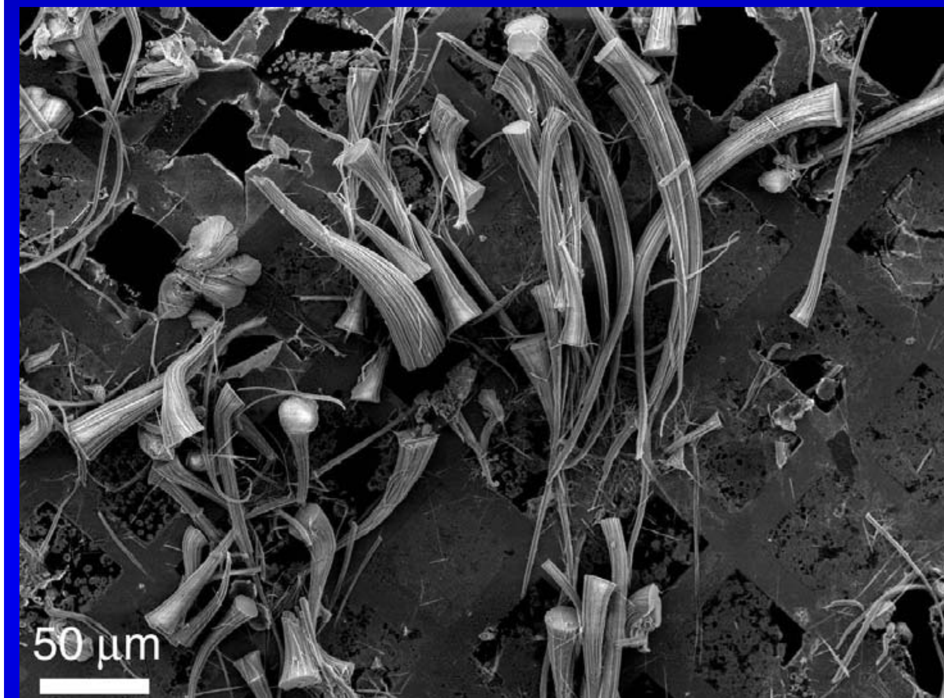

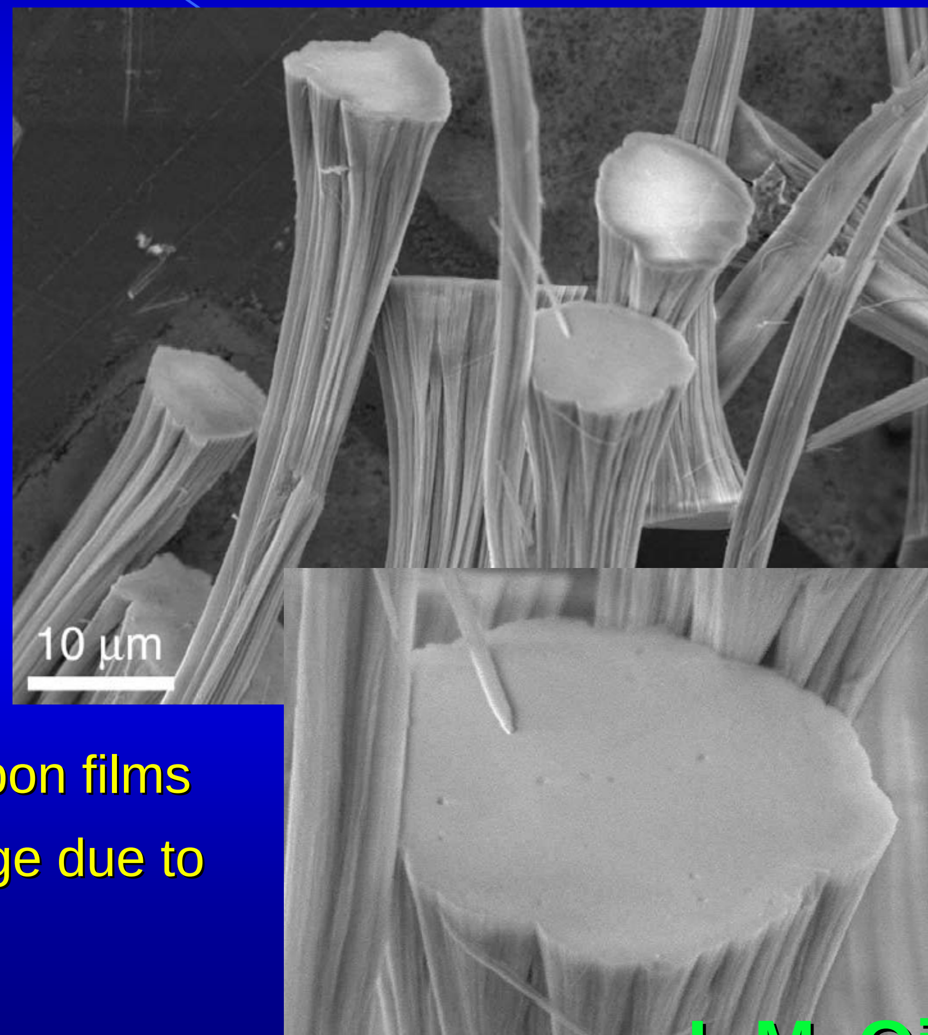

- Heterogeneous nucleation on carbon films
- Perfectly flat surface of growth edge due to surface minimization

L.M. Qi

Crystallographically oriented nanoparticle attachment

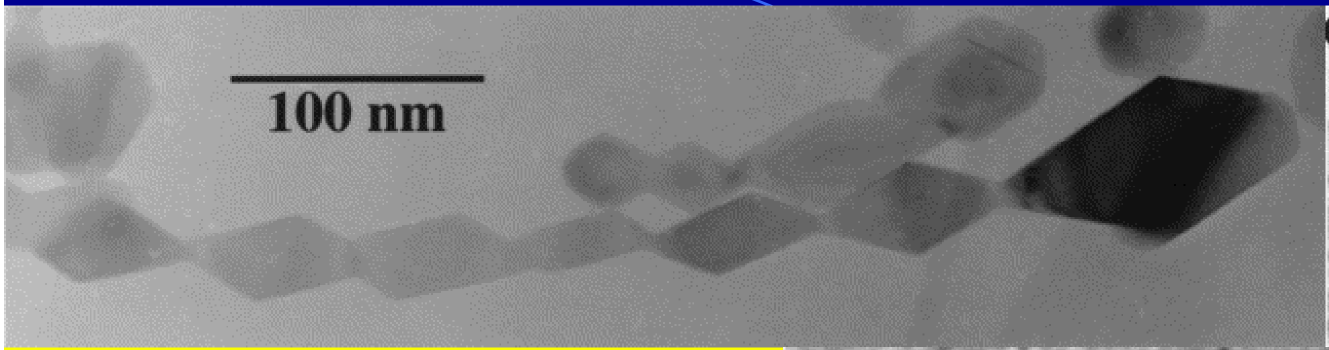

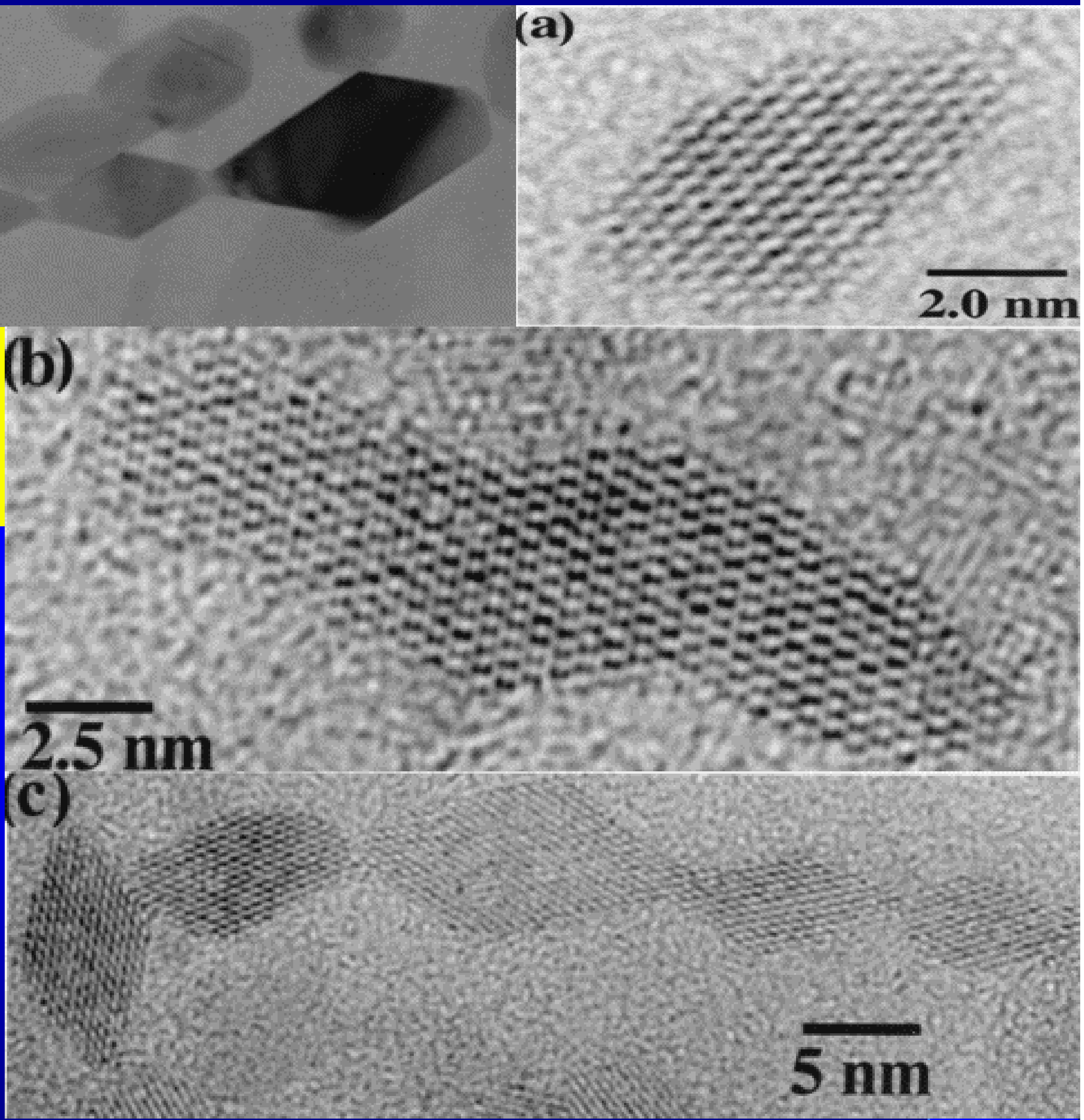

Single crystalline anatase TiO_2 particles hydrothermally synthesized in 0.001 M HCl

Topotactic particle attachment at high energy surfaces (112)

a) Single primary crystal,
b) four primary crystals forming a single crystal via oriented attachment,
c) Single crystalline anatase particle

R.L. Penn, J.F. Banfield; Geochim. Cosmochim. Acta. 63 (1999) 1549 - 1557

L.M. Qi

1)
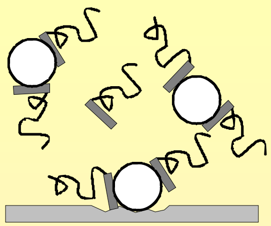

2)
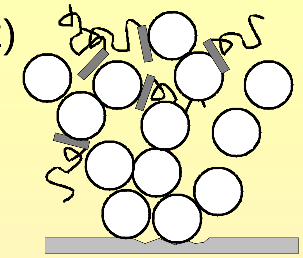

3)
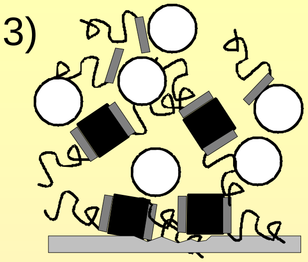

Nucleation of amorphous nanoparticles, polymer stabilization

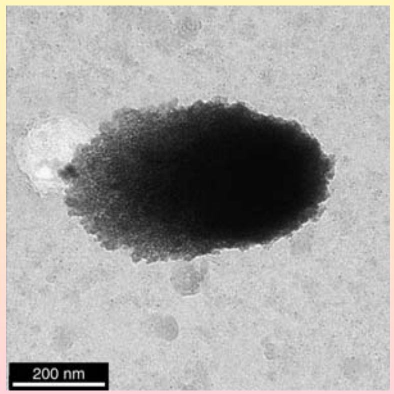

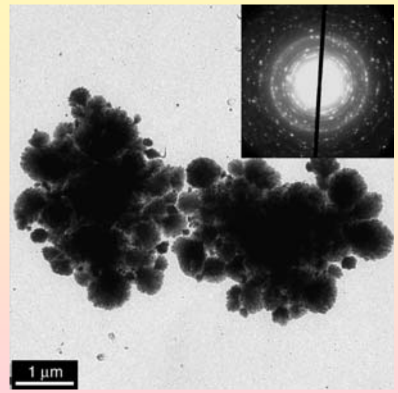

4)
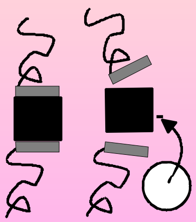

5)
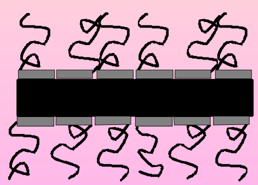

6)
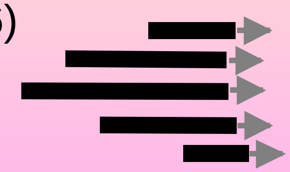

7)
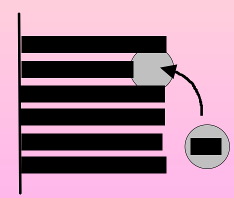

Crystallization of amorphous particles, directed particle fusion

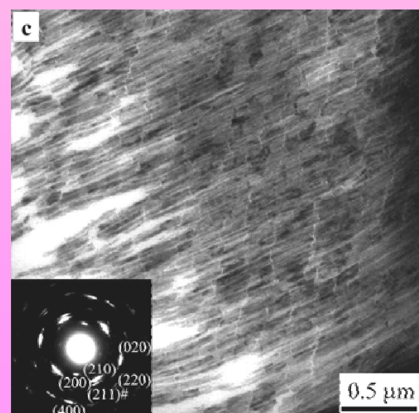

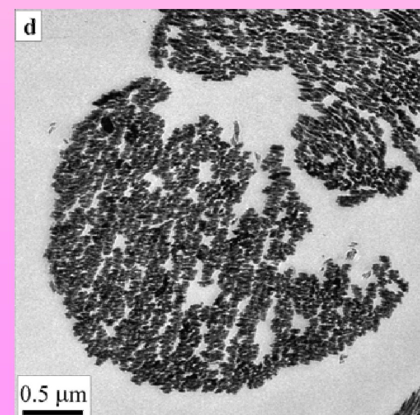

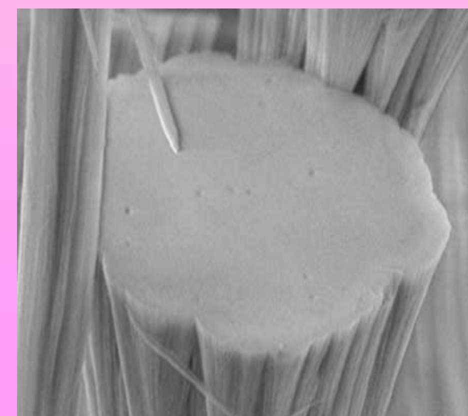

Perfect Single Crystals Fiber Bundles: Elongation along [210]

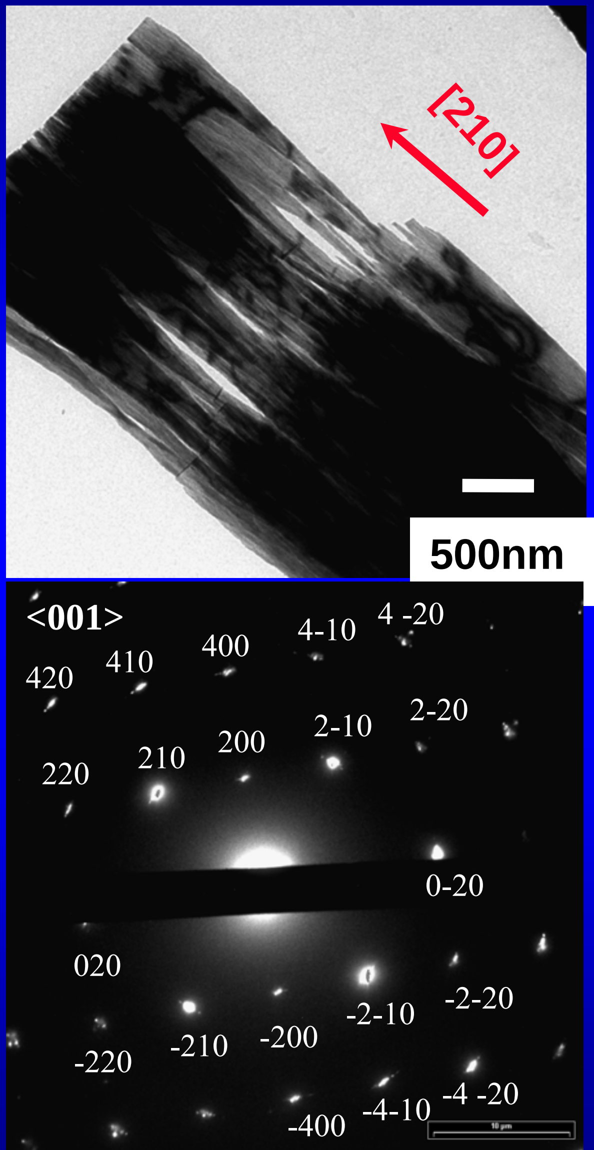

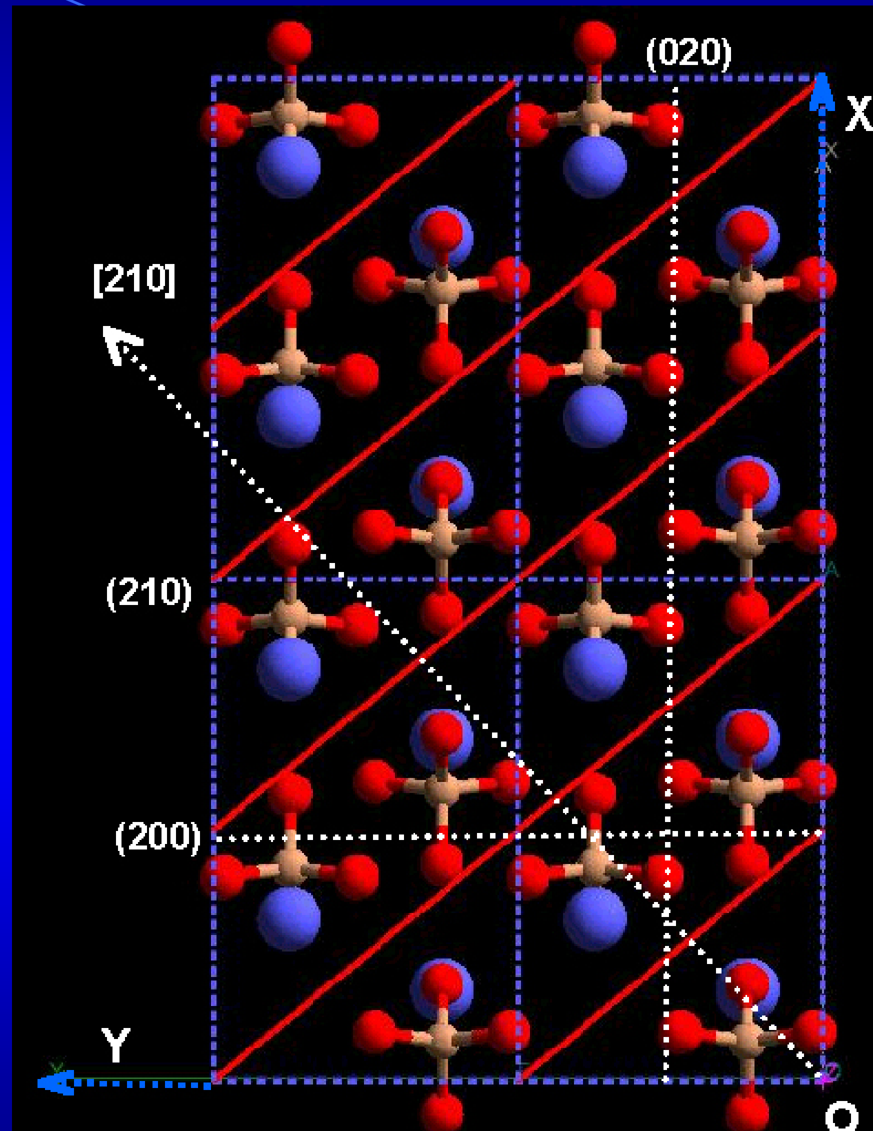

XY projection

S.H. Yu

Structural reconstruction

$BaSO_4$, 2 mM, polyacrylate (Mn = 5100) 0.11mM, pH = 5.5, 25

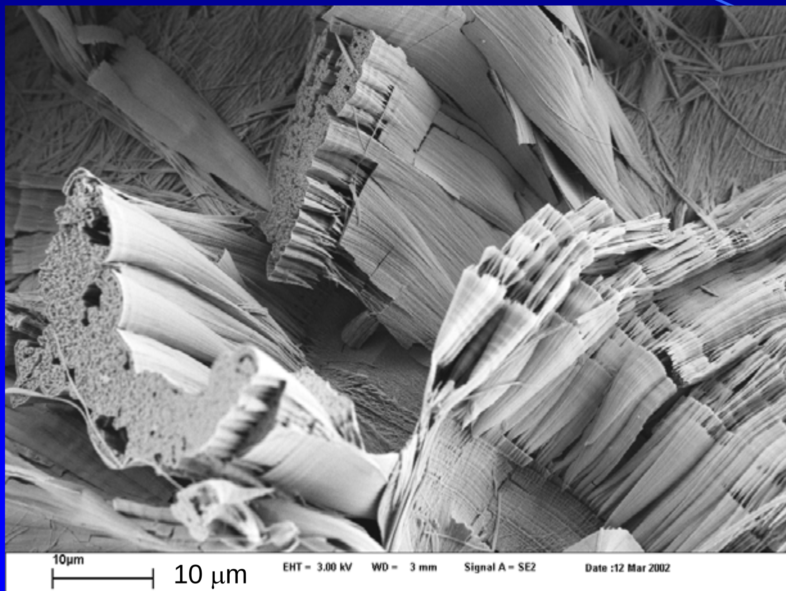

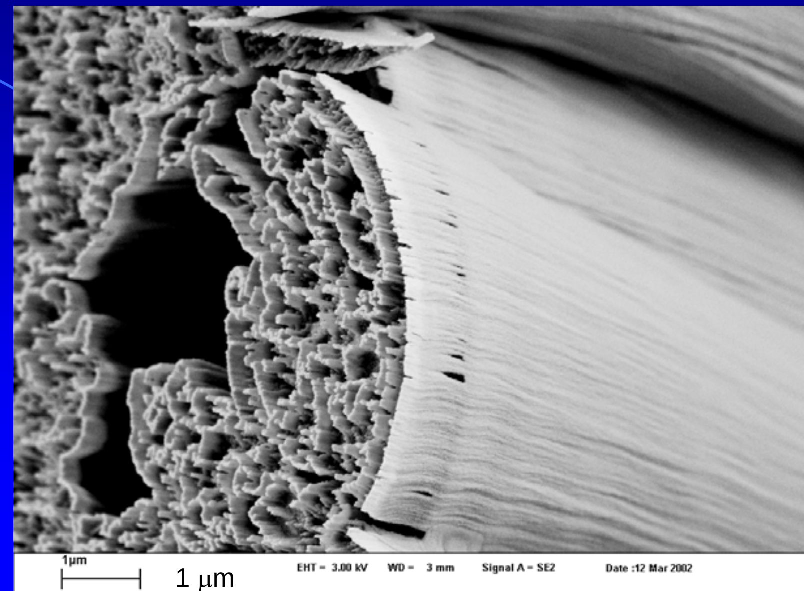

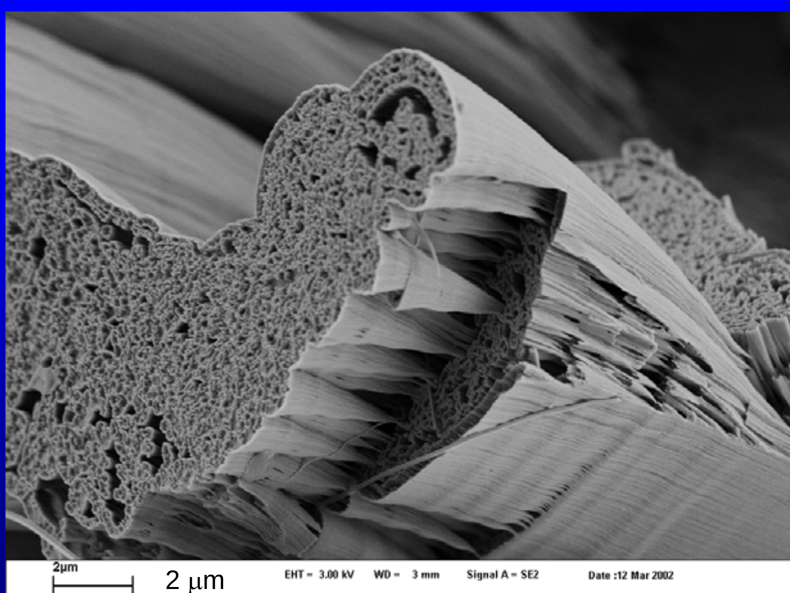

Cuttlefish bone

β-Chitin + aragonite

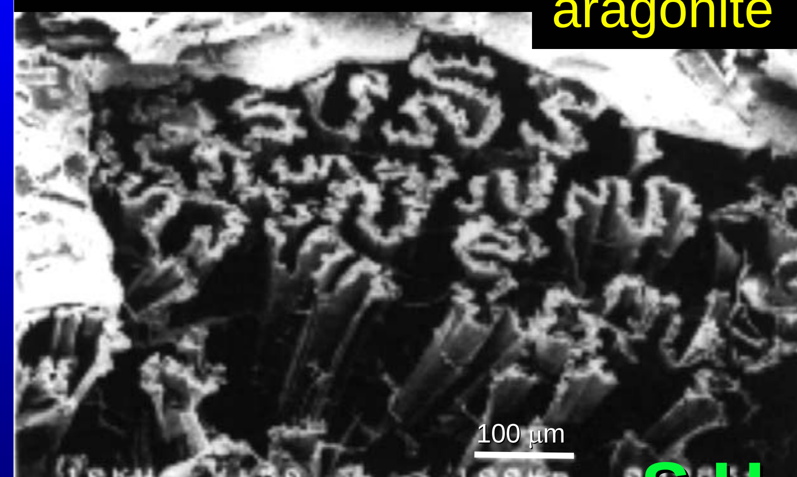

S.H. Yu

Higher order assembly

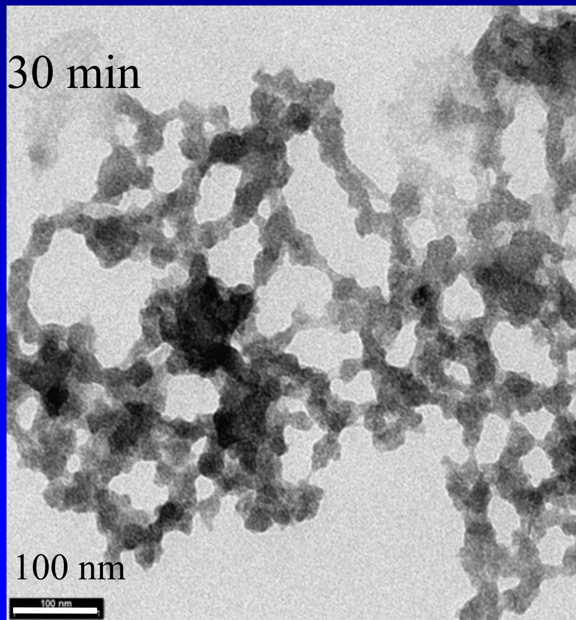

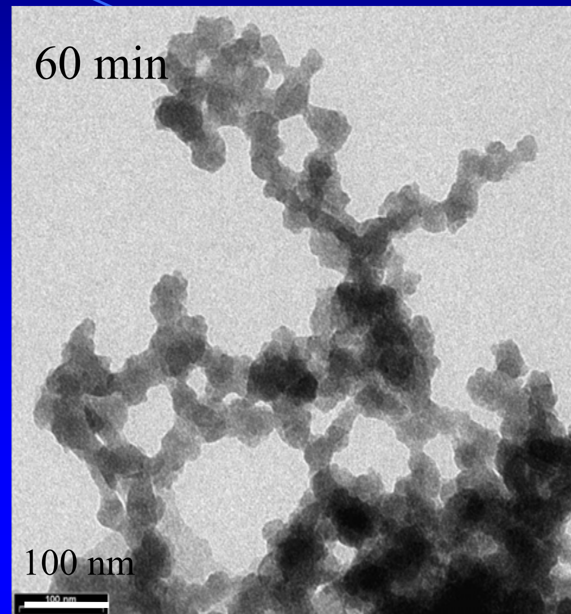

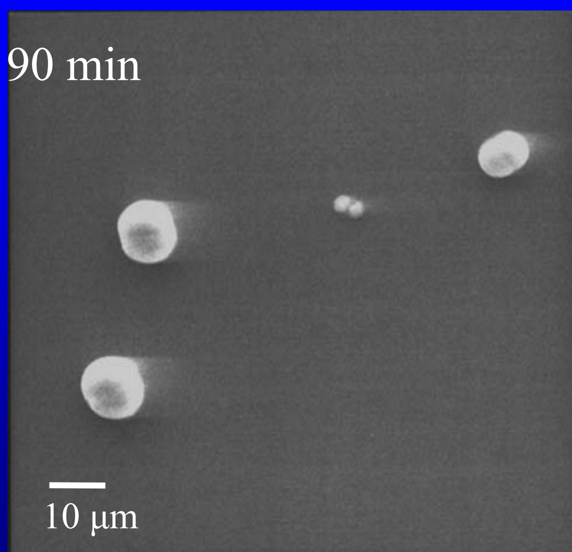

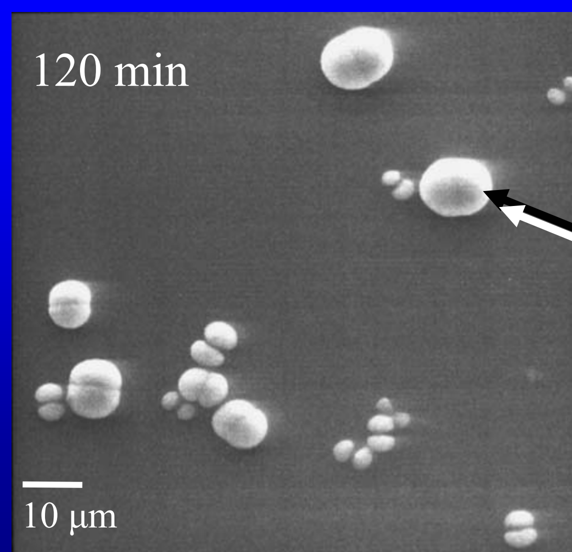

[PEG-b-PMAA] = 1 g/l,
$[CaCO_3]$ = 8 mM,
pH = 10

- Chains of aggregated amorphous nanoparticles
- Dumbbell shaped and spherical aggregates
- Nanoparticle crystallization

Primary crystals 40 nm

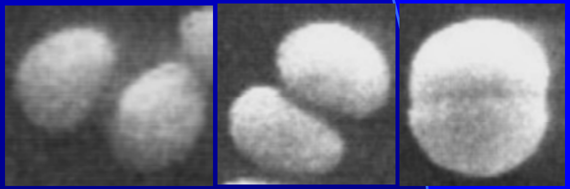

Zoom

L.M. Qi

Light microscopy on $CaCO_3$ with PEO-b-PMAA

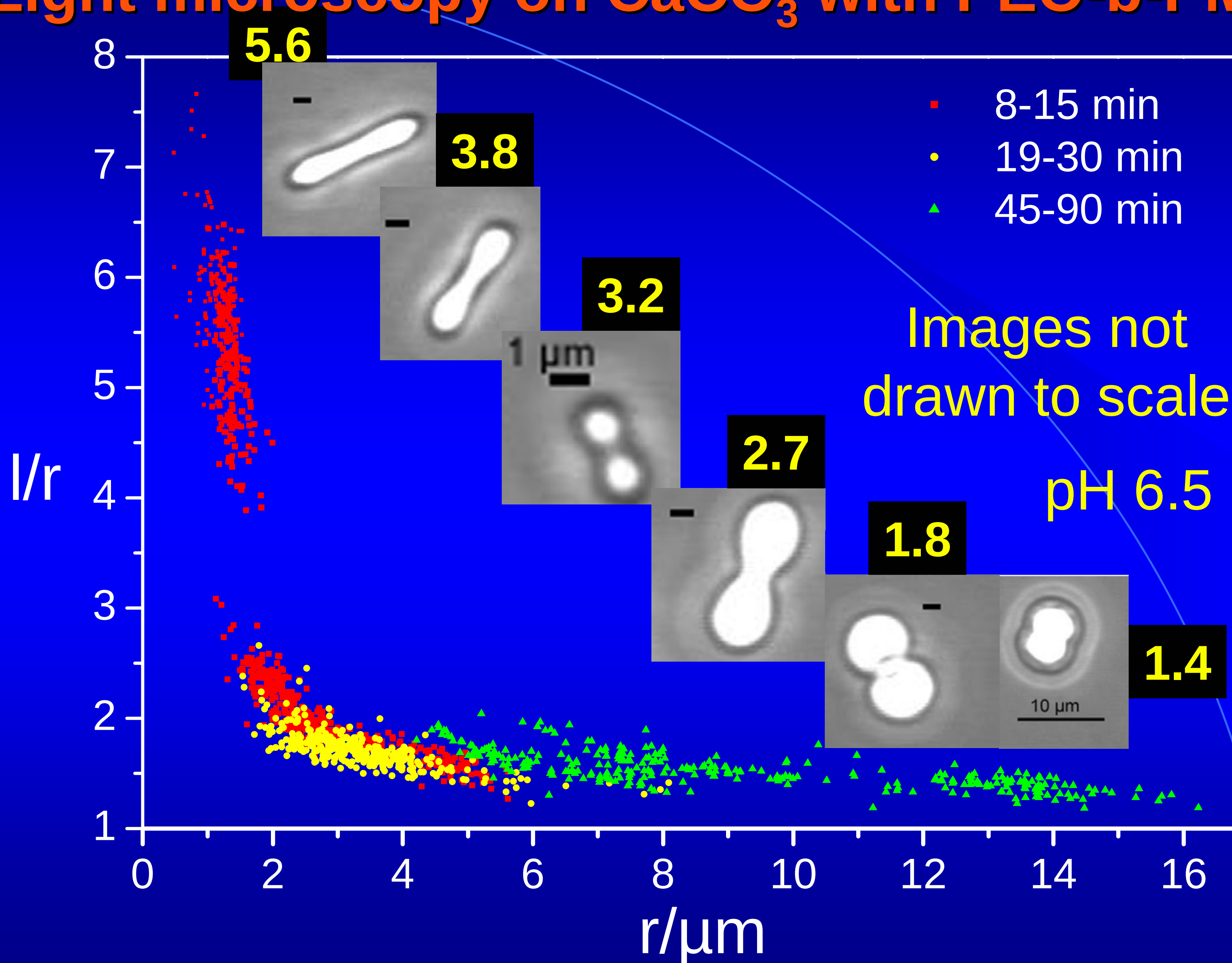

A. Reinecke, H.G. Döbereiner

Higher order assembly

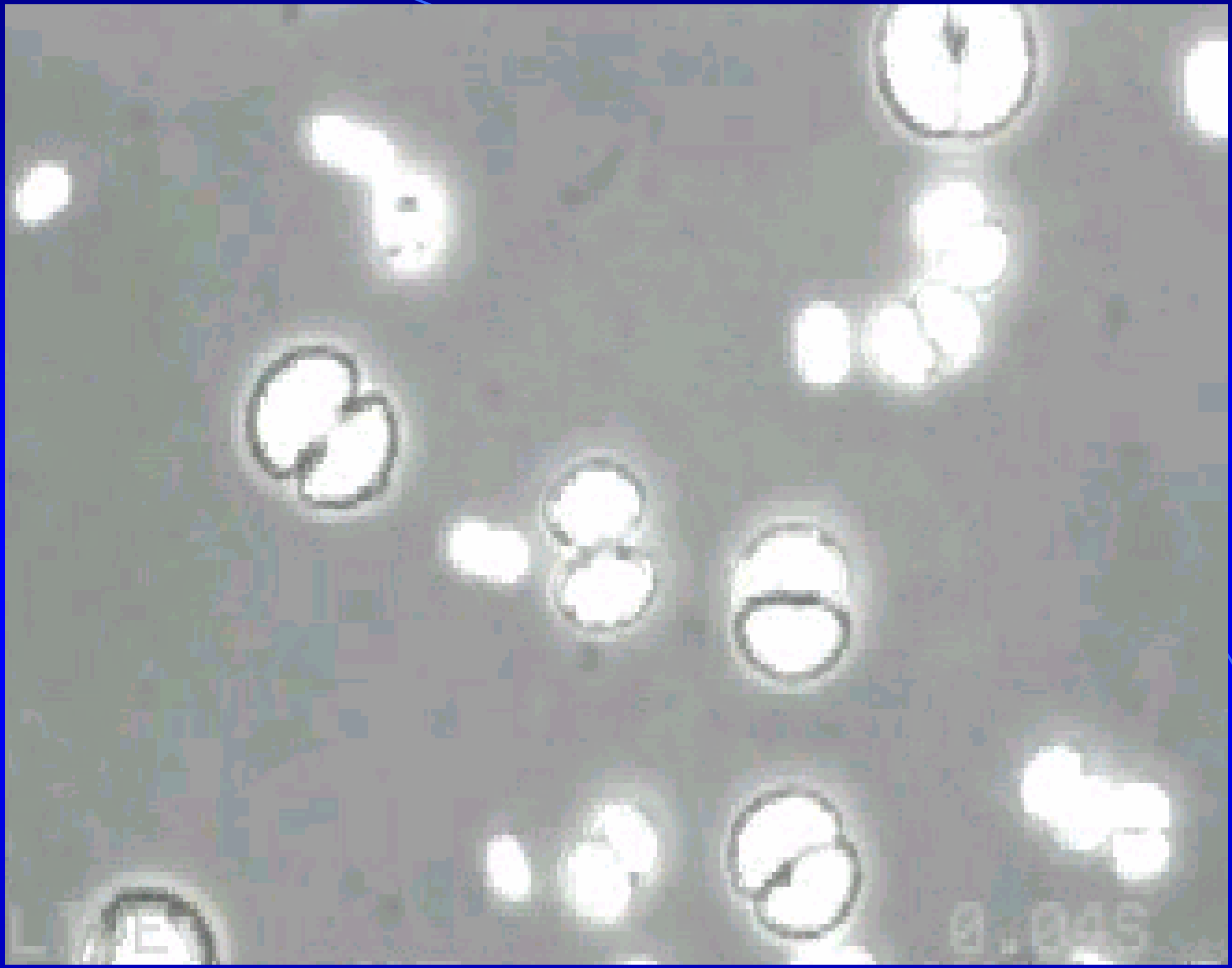

Aggregate structures are also observed if the crystals are dissoved with HCl

A. Reinecke, H.G. Döbereiner

Higher order assembly

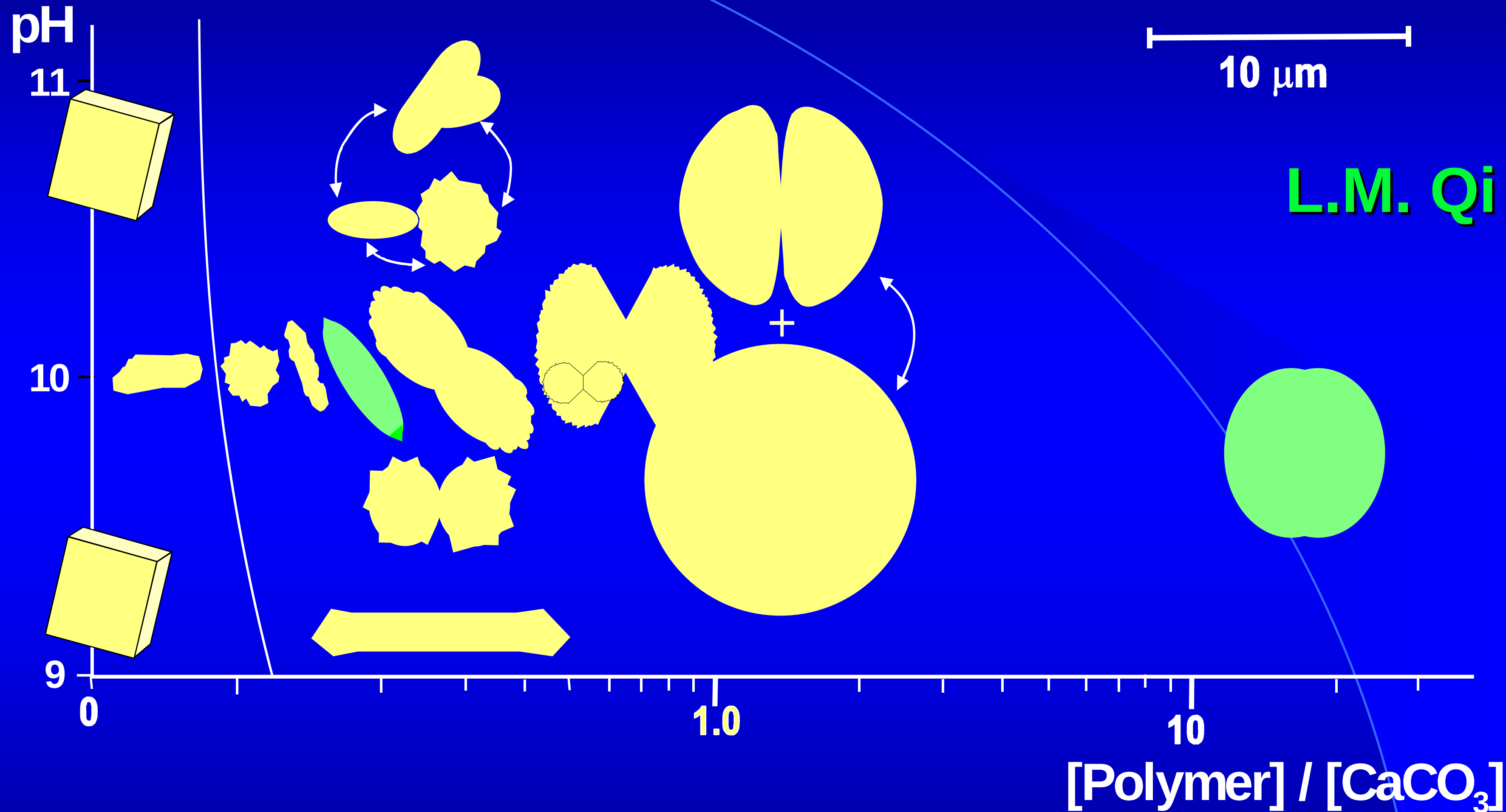

L.M. Qi

- Supersaturation and strength of polymer-mineral interaction (pH) and [Polymer] / [$CaCO_3$] play important role for morphogenesis

Higher order assembly

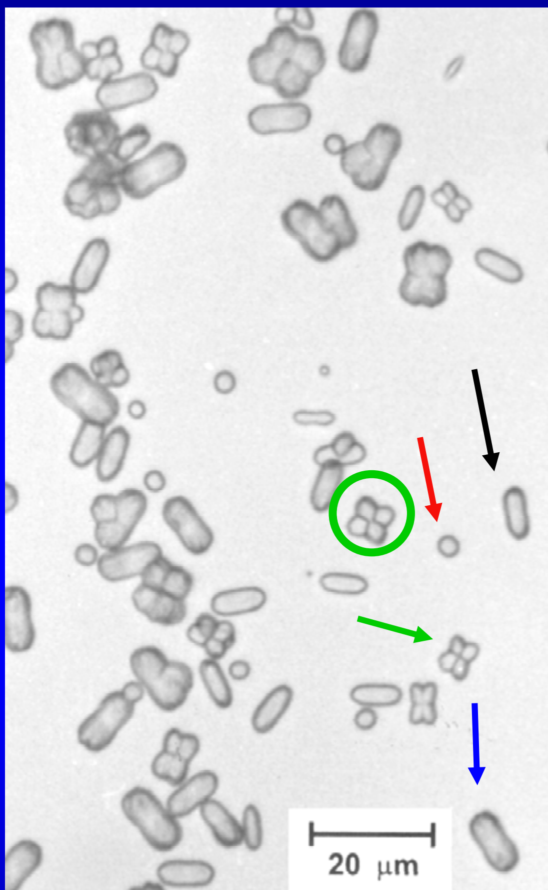

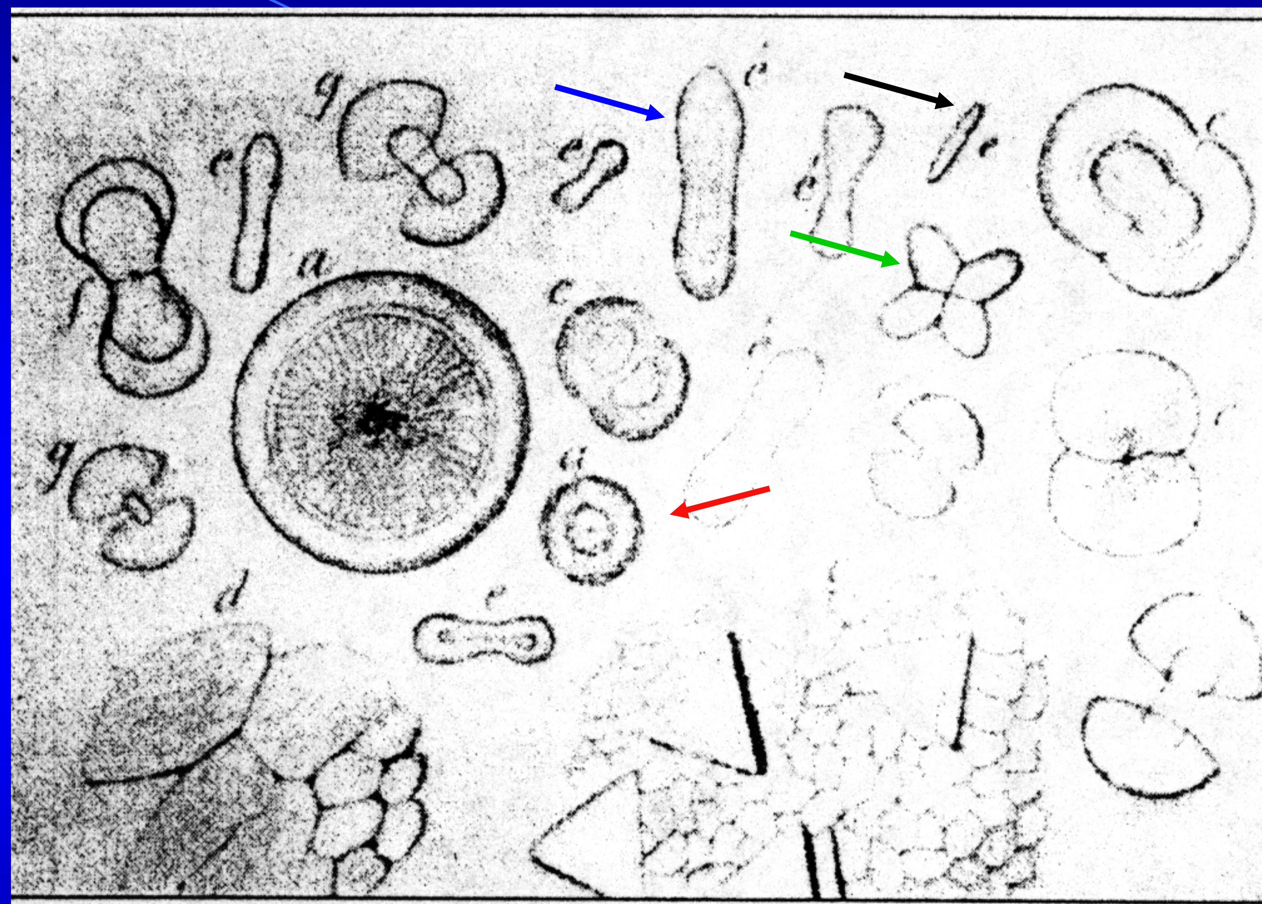

$CaCO_3$ +
PEG-*b*-PEDTA-$C_{17}H_{35}$
Composed of nanoparticles

$CaCO_3$ in oyster marrow matrix
P. Harting 1873

M. Sedlak

Higher order assembly

L.M. Qi

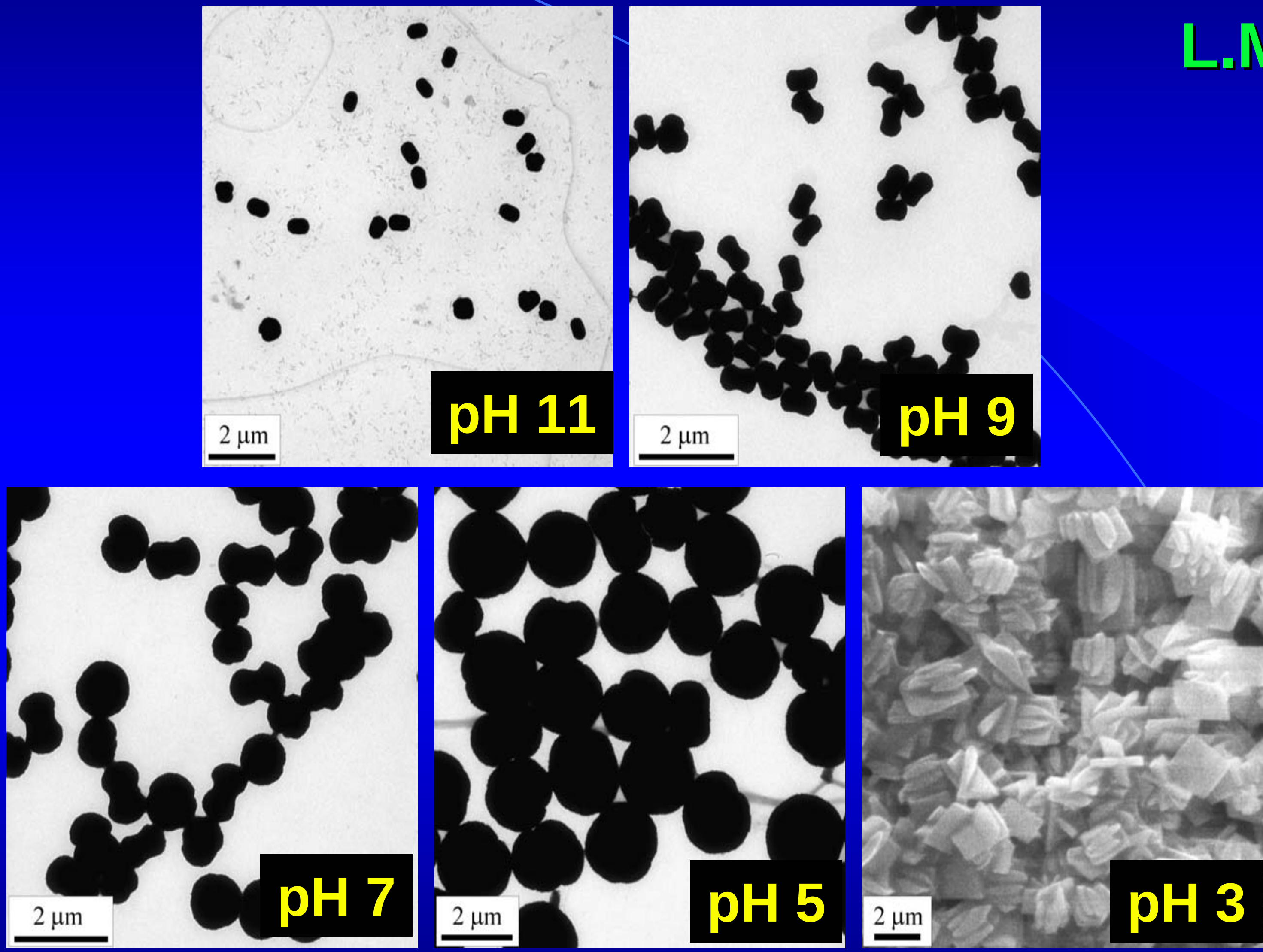

$BaSO_4$ with PEG-*b*-PMAA additive; pH variation

$BaCO_3$ Morphogenesis

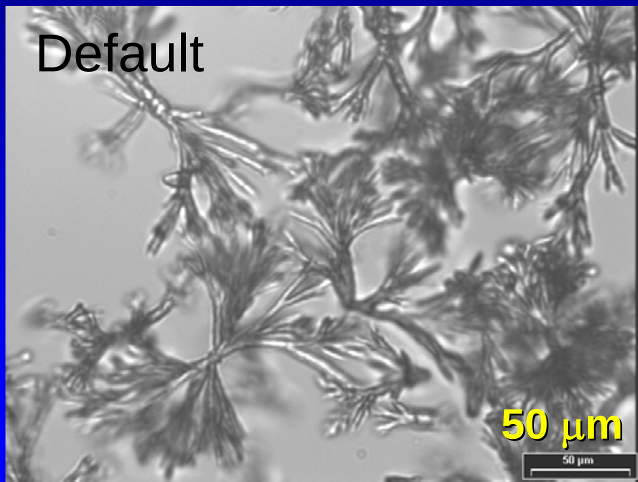

$BaCO_3$ + PEG-*b*-PMAA (1g/L), Ba^{2+} = 10 mM, gas-diffusion reaction, 2 days

Different growth stages from rods (1), growth at the ends (2), via dumbbells (3) to spheres (4).

Apparently no directed nanoparticle assembly but dendritic radial outgrowth.

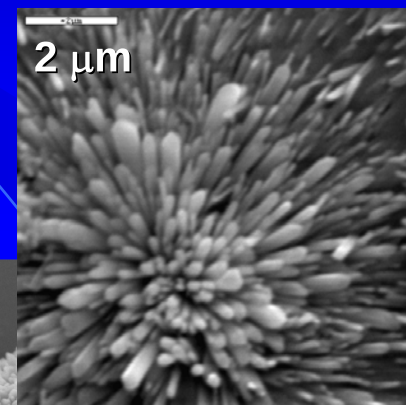

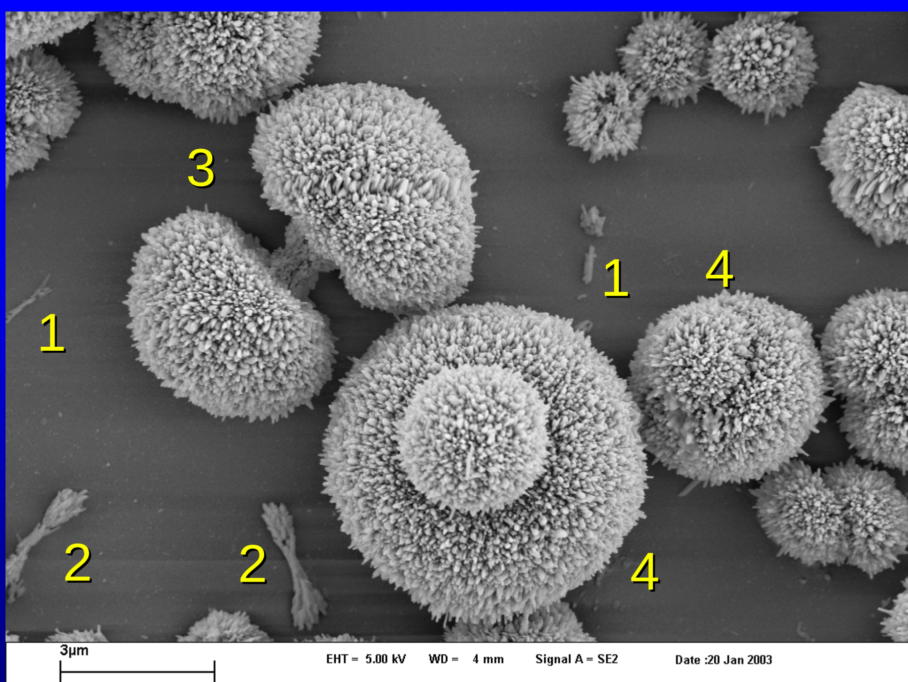

3 µm

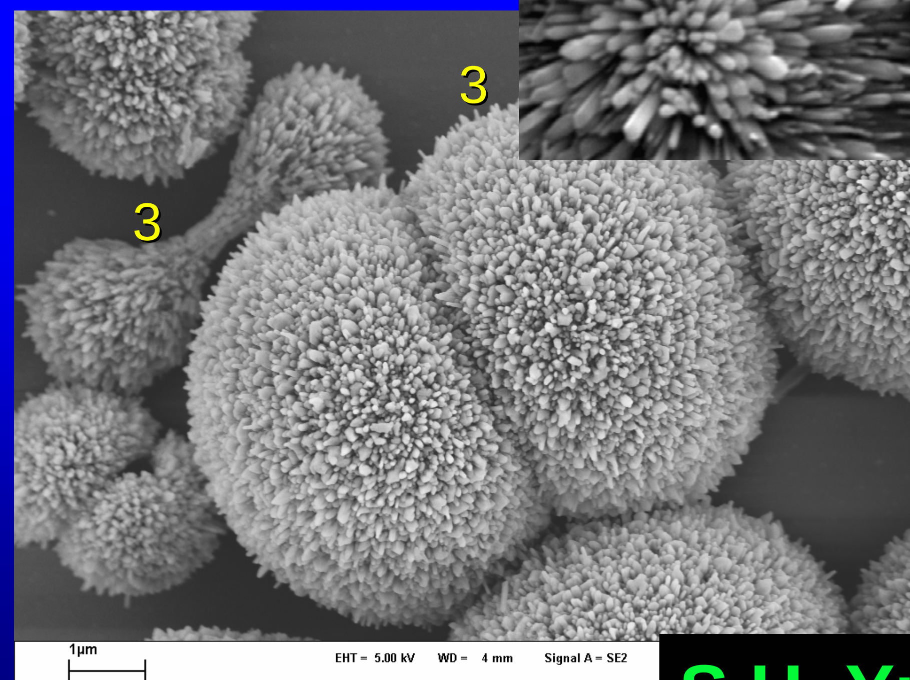

1 µm

S.H. Yu

Chirality introduction by a racemic polymer

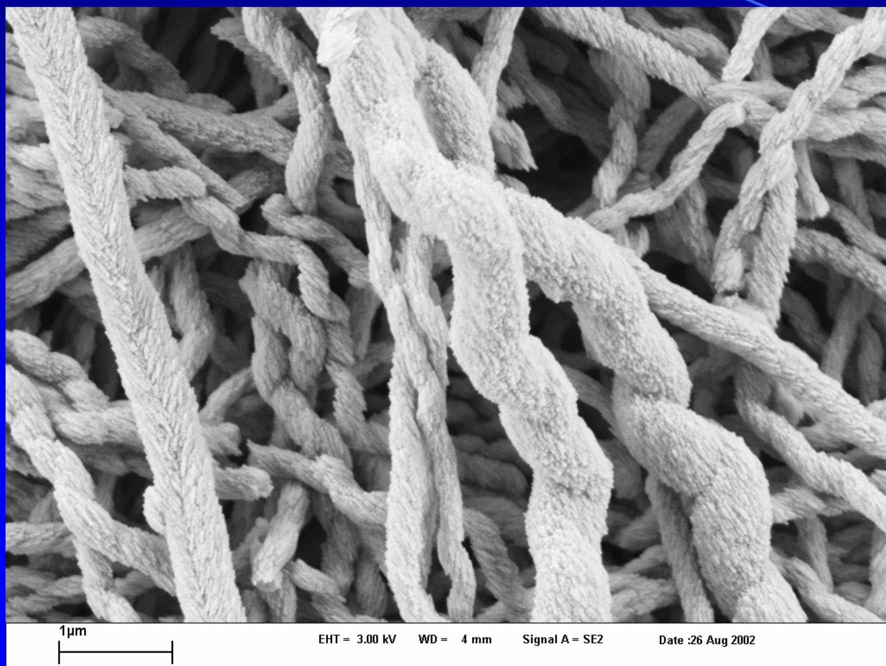

1 g L^{-1}, pH = 4, [$BaCl_2$] = 10 mM, on glass slip, gas diffusion reaction

14 d

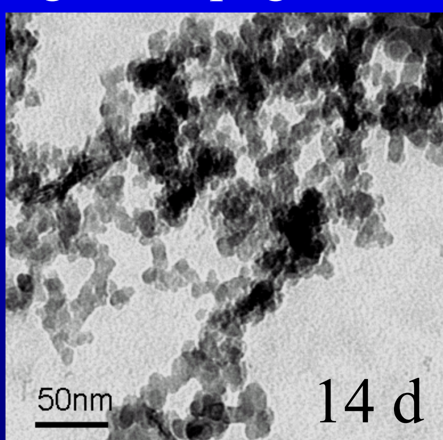

Amorphous precursor after 5h

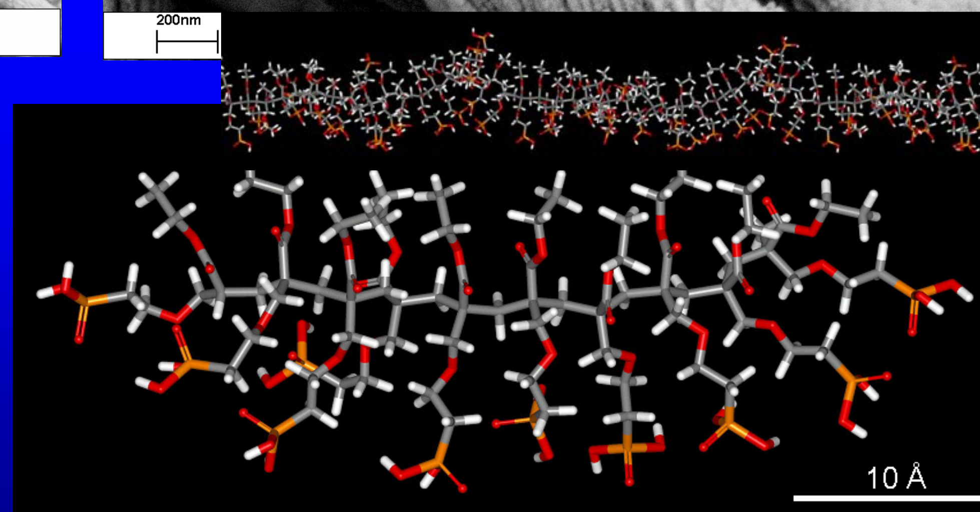

PEG-*b*-[(2-[4-Dihydroxy phosphoryl)-2-oxabutyl) acrylate ethyl ester,
M_w = 120000 g/mol, PEO = 2000 g/mol

$BaCO_3$ orthorhombic crystal structure

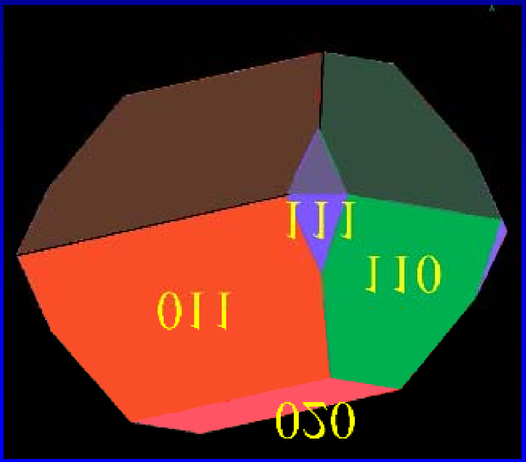

Vacuum equilibrium morphology

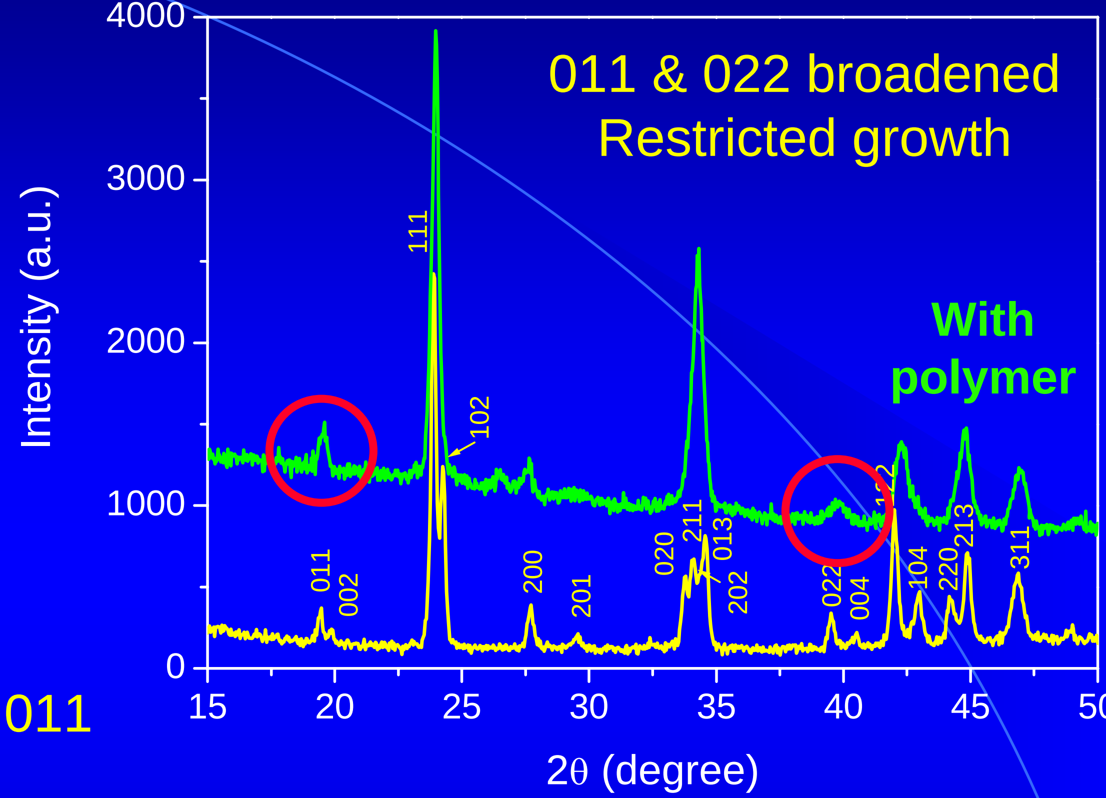

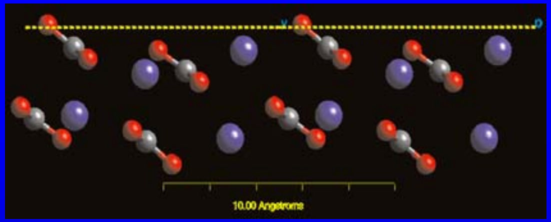

011

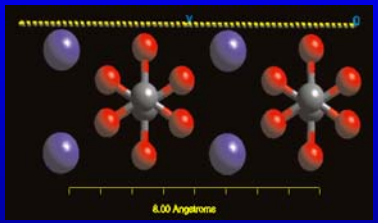

020

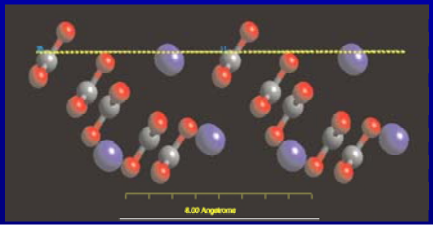

111

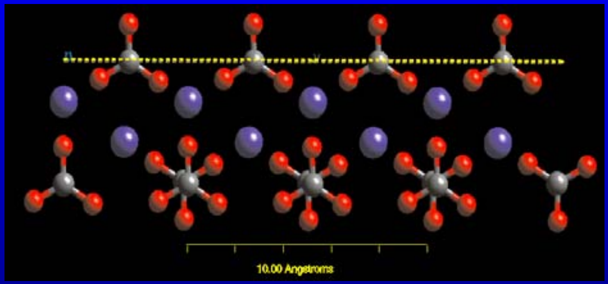

110 favourable for polymer interaction

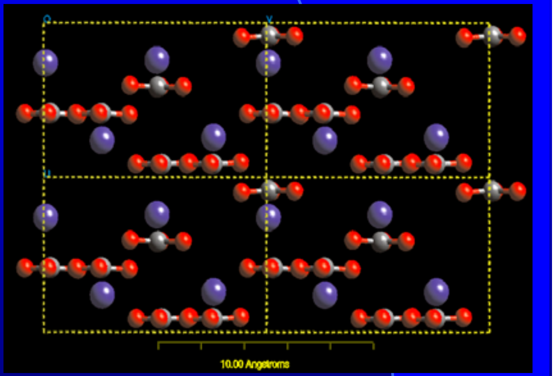

S.H. Yu, K. Tauer

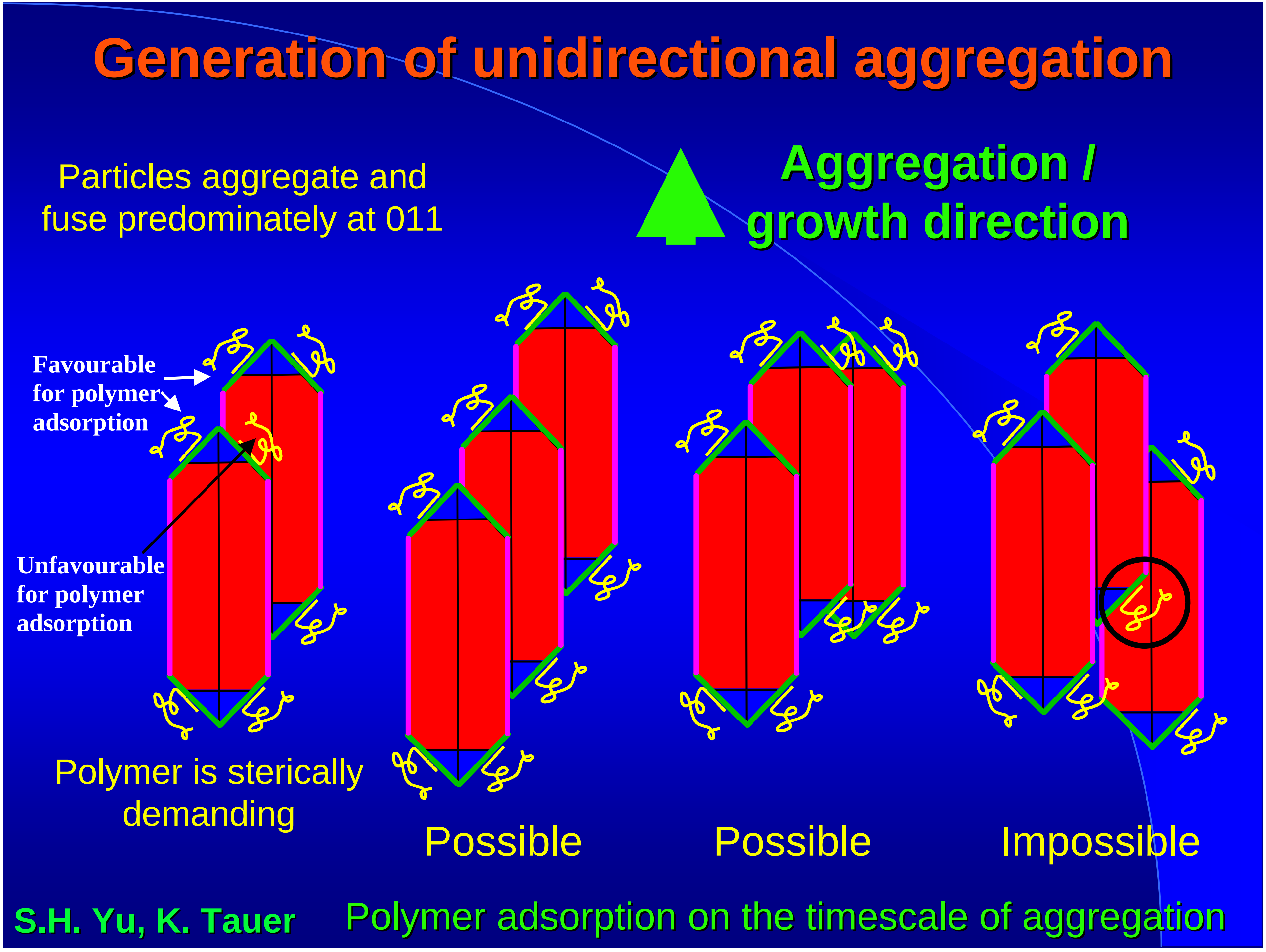
Generation of unidirectional aggregation
Particles aggregate and fuse predominately at 011
Aggregation / growth direction
Favourable for polymer adsorption
Unfavourable for polymer adsorption
Polymer is sterically demanding
Possible
Possible
Impossible
S.H. Yu, K. Tauer
Polymer adsorption on the timescale of aggregation

Chirality introduction by a racemic polymer

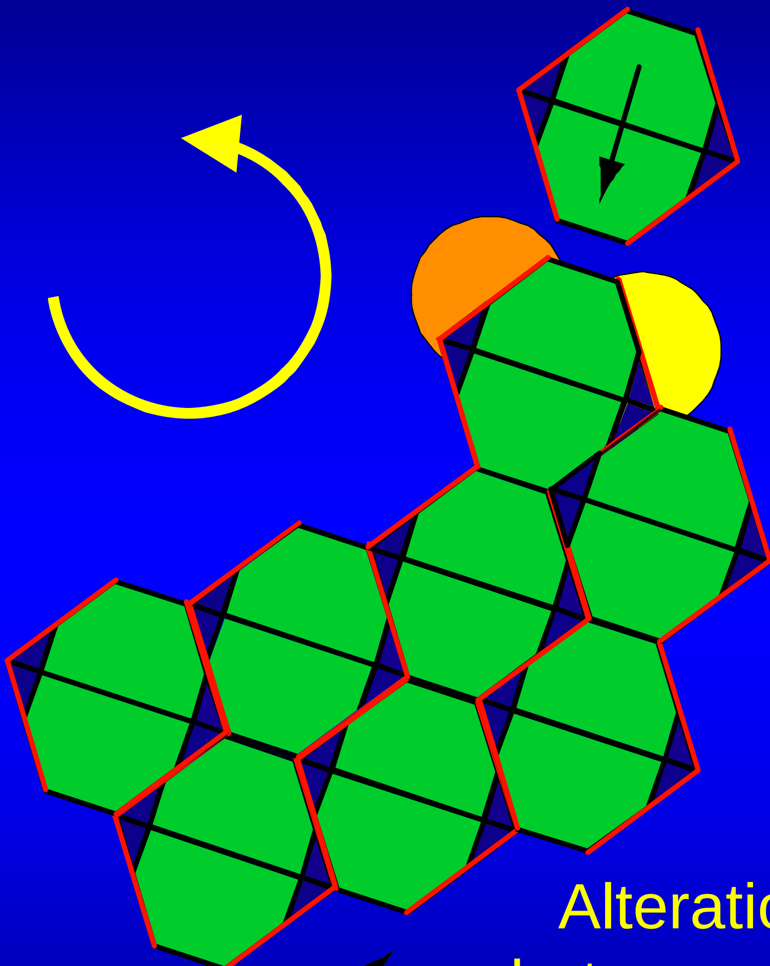

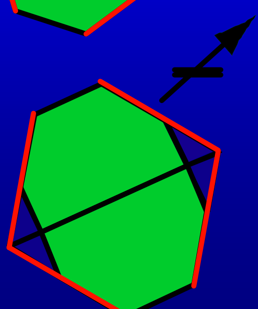

Alteration between 020 and 011 aggregation creates turn

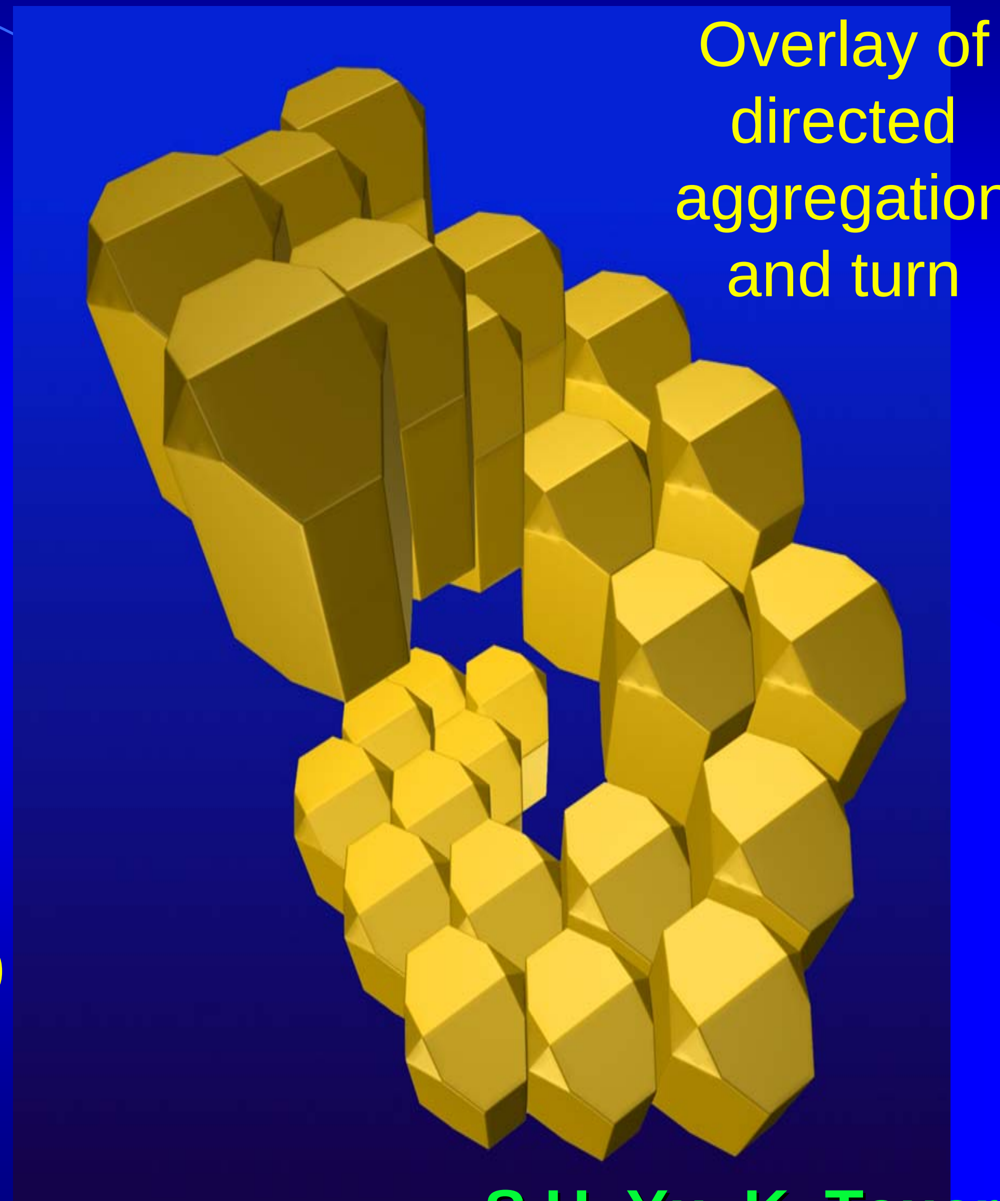

S.H. Yu, K. Tauer

Control experiments on mechanism

Increase lateral growth

Particle attachment prevails over polymer adsorption.

Polymer 1 g L^{-1}, pH = 5.6, Less particle charge as IEP = 10.0 – 10.5

Decrease lateral growth

Polymer adsorption prevails over particle attachment.

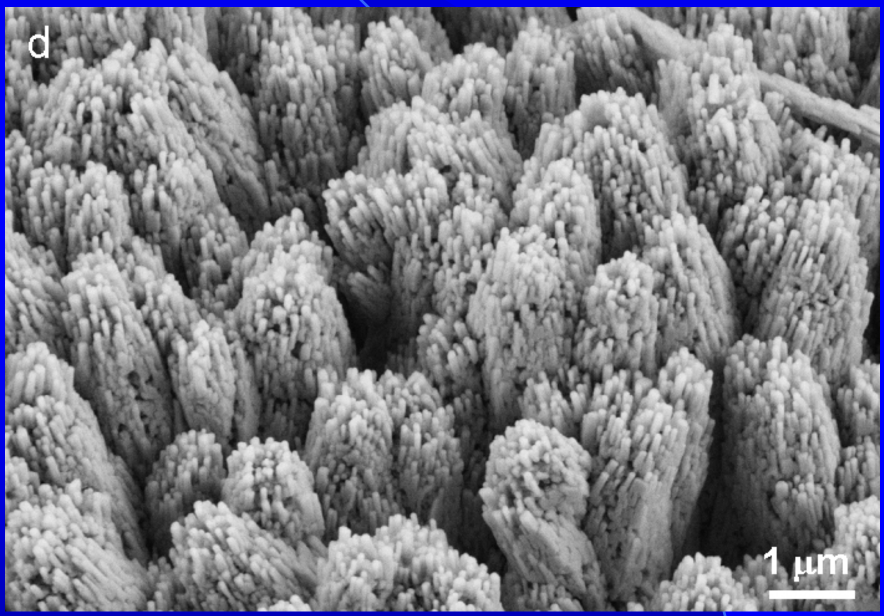

Polymer 2 g L^{-1}, pH = 4, $[BaCl_2]$ = 10 mM

S.H. Yu, K. Tauer

Organic Mesocrystals, the D,L-Alanin example

Default

Supersaturated solution at 65 °C cooled to 20 °C

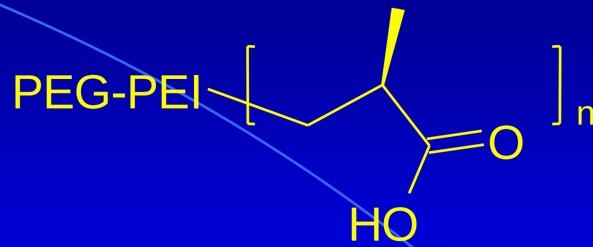

41 % functionalization

$c_{Polymer}$ = 1 g/l

PEG-*b*-PEI-*s*-But-COOH

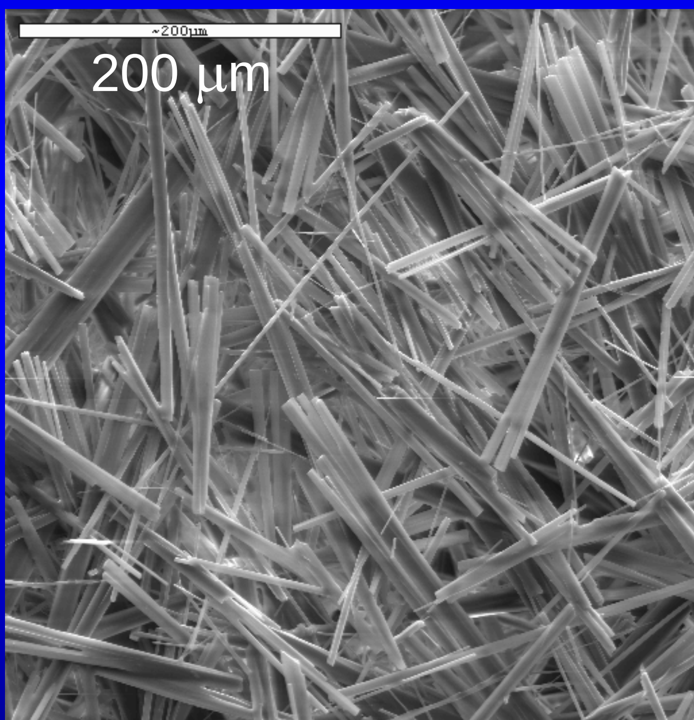

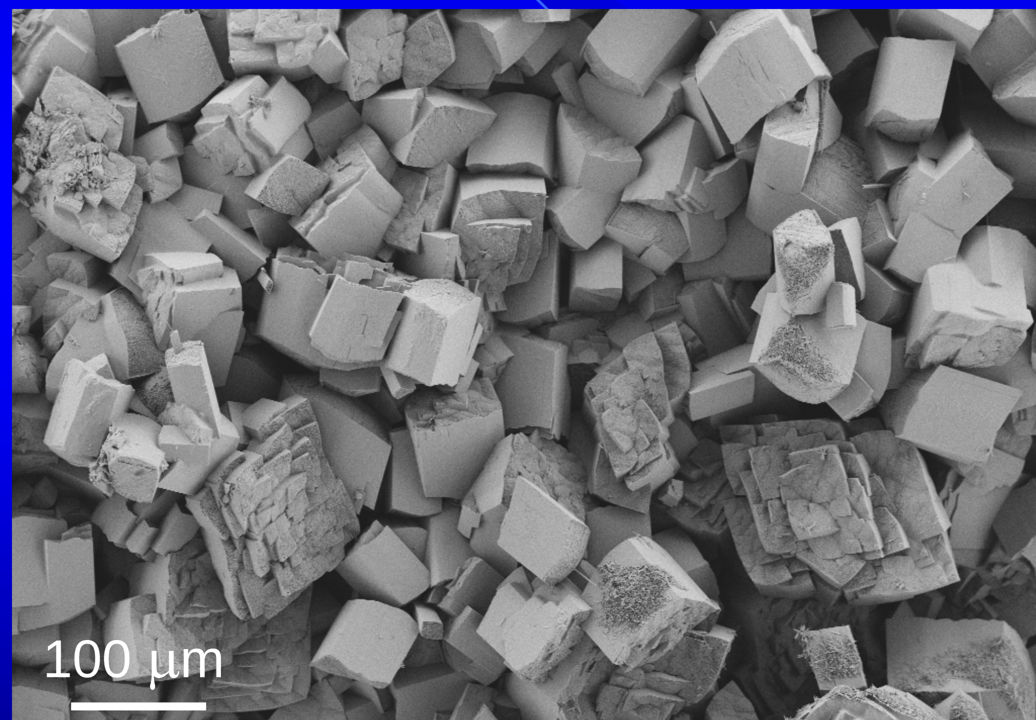

S. Wohlrab

Organic Mesocrystals, the D,L-Alanin example

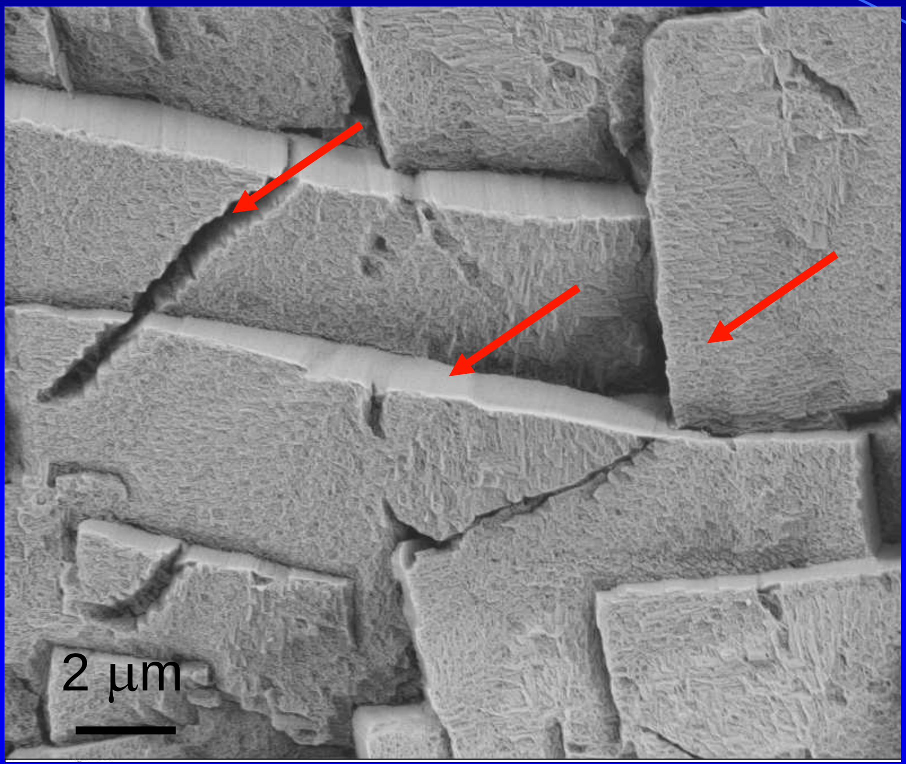

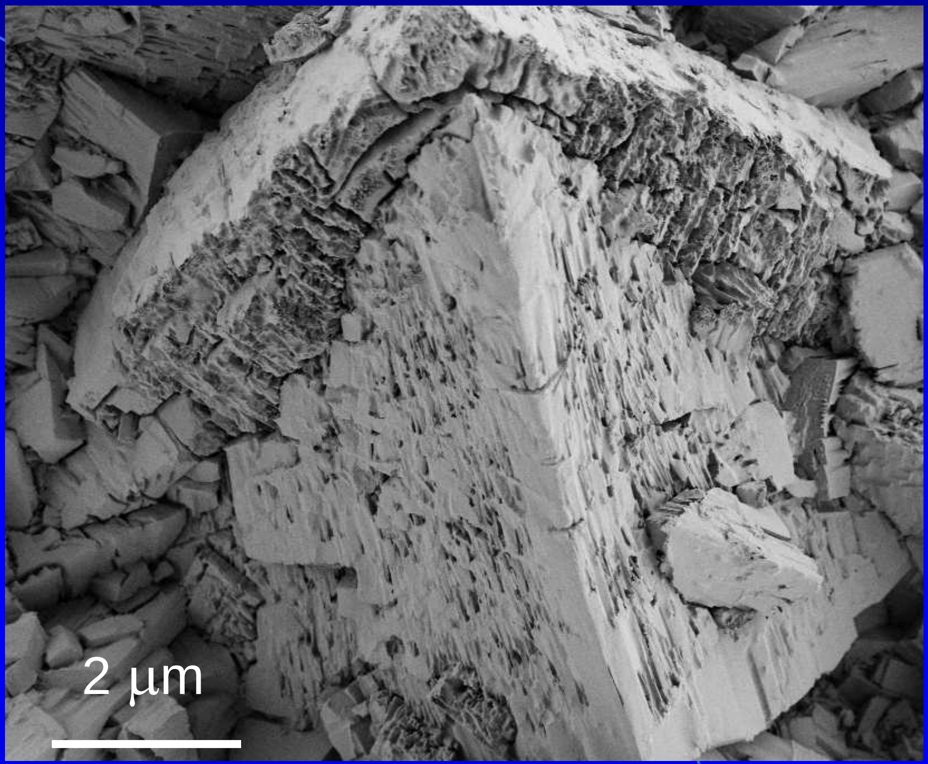

Crystalline appearance but:

- Rough and even surfaces
- Nonplanar surfaces
- Cracks indicate swollen structure

Partial polymer dissolution after boiling in MeOH indicates hybrid structure

S. Wohlrab

D,L Alanin + 1 g/l PEG-*b*-PEI-s-But-COOH

Organic Mesocrystals, the D,L-Alanin example

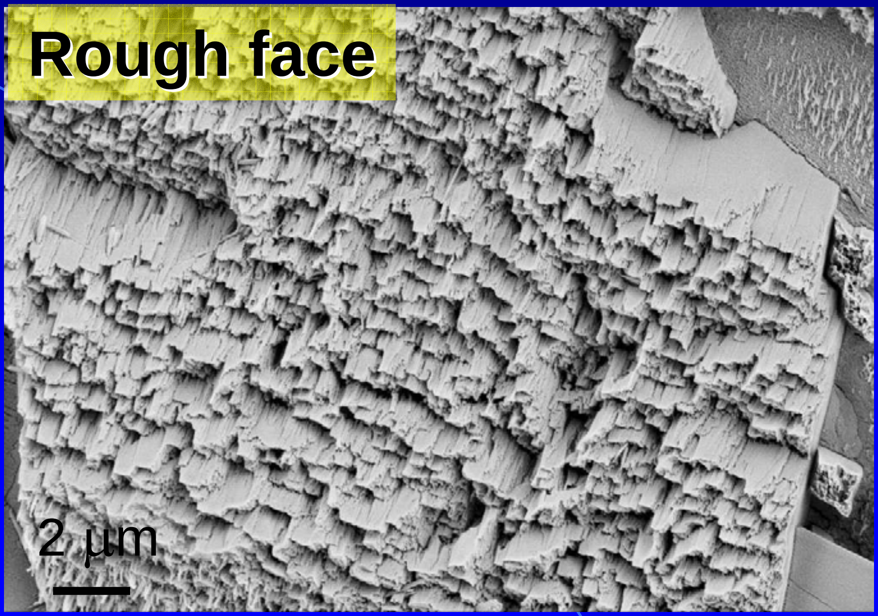

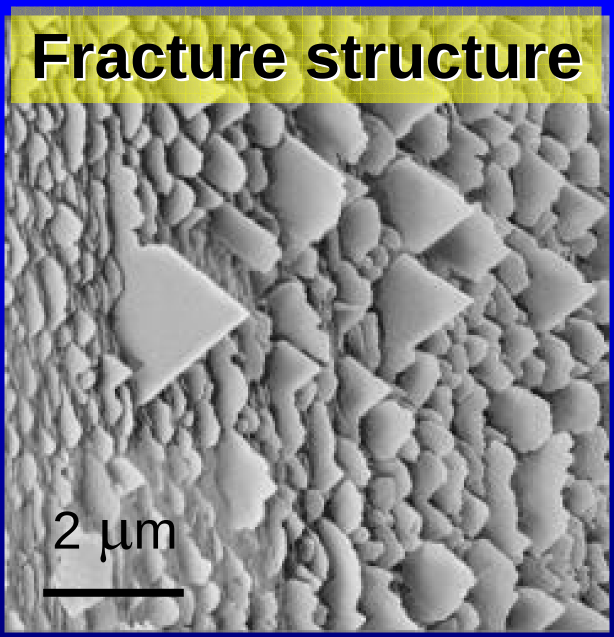

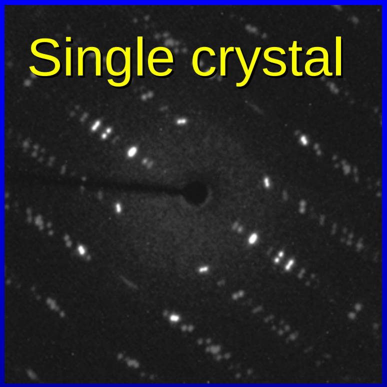

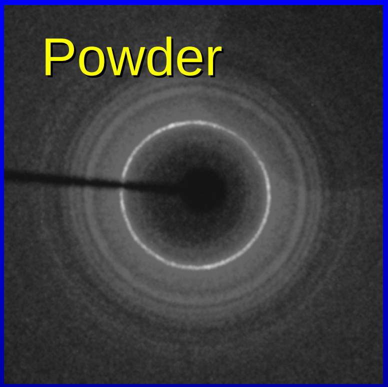

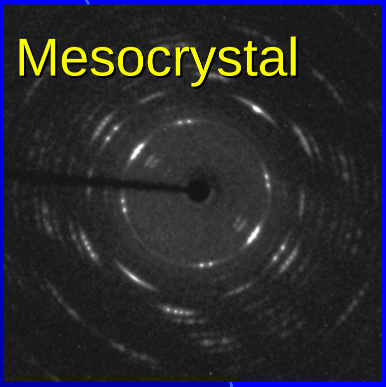

X-ray single crystal analysis

D,L Alanin + 10 g/l
PEG-*b*-PEI-s-But-COOH

S. Wohlrab

Different modes of cyrstal growth

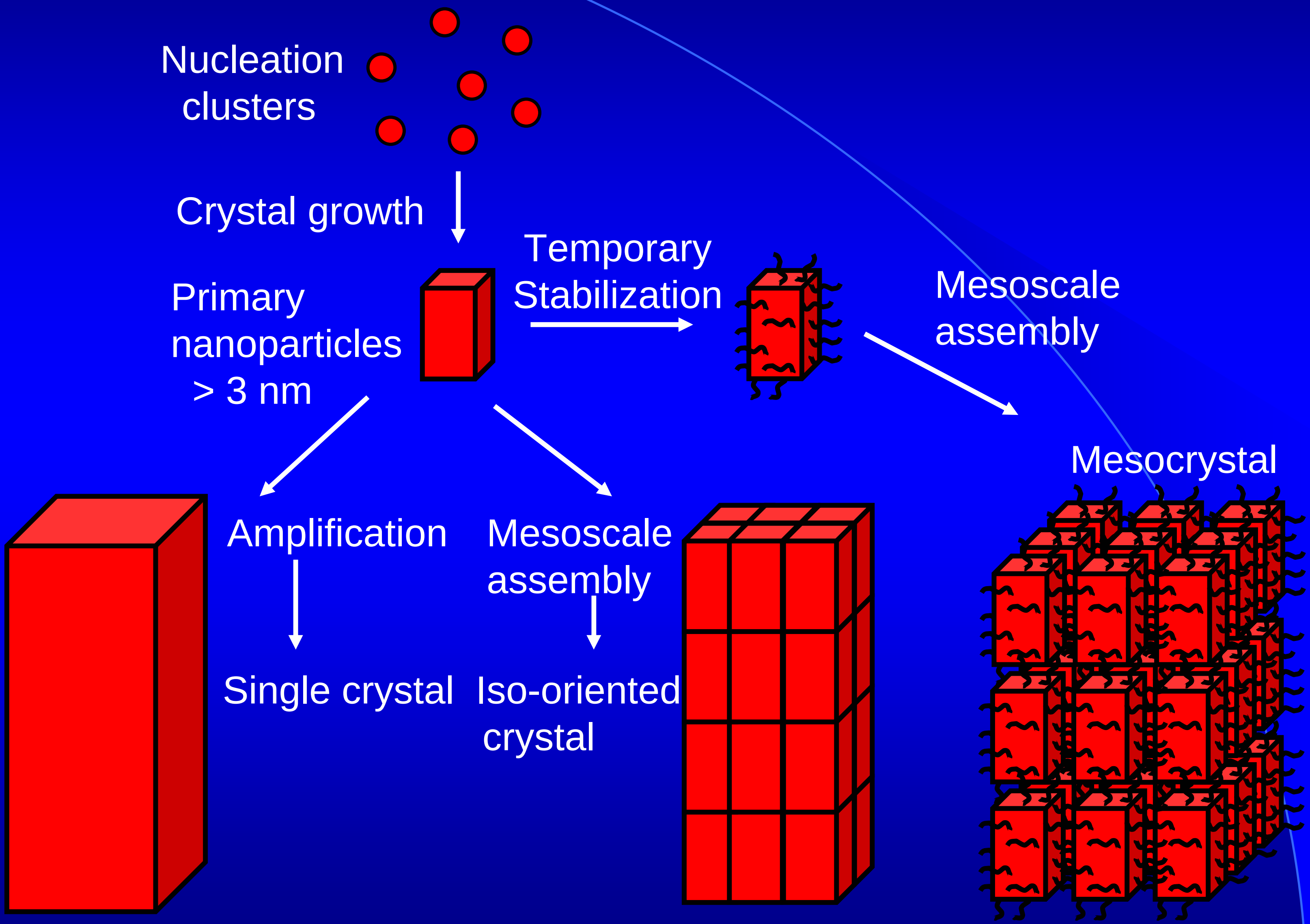

Organic Mesocrystals, the D,L-Alanin example

D,L Alanin + 1 g/l PEG-*b*-PEI-s-But-COOH + NaCl

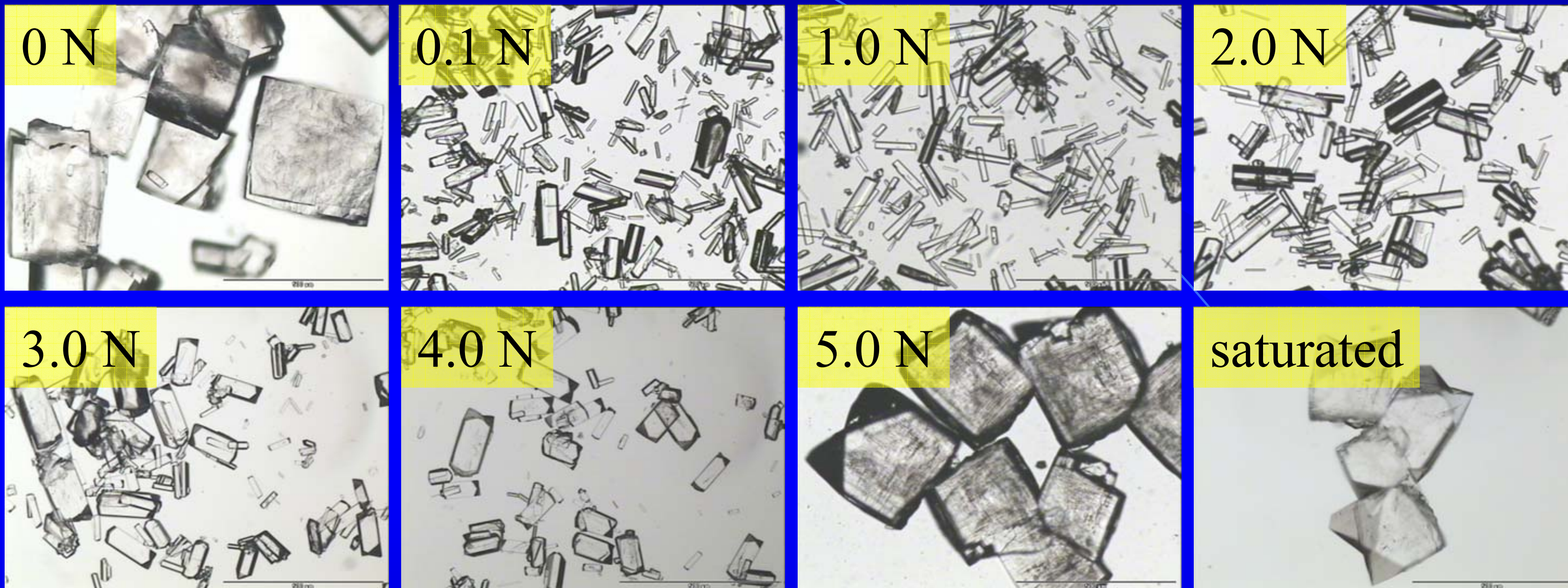

Salt addition dramatically changes the mesocrystal morphology

- **Counterplay between electrostatic & vdW forces**
- **Polymers attach to different surfaces**
- **D,L Alanin molecule is already a dipole !**

S. Wohlrab

Conclusions

- Bio-inspired mineralization can transfer biomineralization principles towards the synthesis of advanced organic-inorganic hybrid materials at ambient temperature in water.
- Self-assembled superstructures can be generated by tuneable interacting organic block copolymer additives. But: Self assembly only possible up to the micron scale (Need for macroscopic templates)
- Up to now, synergistic effects as often present in biomineralization processes cannot yet be applied in bio-inspired mineralization. Bio-inspired mineralization has still the character of a model system.
- Structure formation mechanisms are still often unknown due to demanding analytics.
- Principles can be extended to organic crystals exploiting new variables like chirality or inherent molecular dipoles.

Bio-inspired mineralization offers a large playground for future materials

Conclusions

- Bio- and biomimetic mineralization offer many indications for non-classical crystallization routes e.g. a crystal is not always built up from ions or molecules but by precursor particles via mesoscopic transformations
- Mesocrystals can be isolated for organic crystals with low lattice energy, for the inorganic counterparts, the lattice energy is too high and forces crystallite fusion with resulting defect structures
- Often, amorphous precursors are observed and mesoscopic transformation generally plays an important role in the final alignment of the crystallites.
- Coding of crystal surfaces by additives can alter the mesocrystal structure and thus the structure of the final single crystal (additive inclusions)

Recommended reading

- S. Mann, *Biomineralization*, Oxford University Press, Oxford, **2001**
- S. Mann, J. Webb, R. J. P. Williams, Biomineralization: Chemical and biochemical perspectives, VCH Weinheim, **1989**
- S. Weiner, *CRC Critical Reviews in Biochemistry,* **1986***, 20,* 365 - 408
- H. Cölfen, S. Mann, *Angew. Chem. Int. Edit.* **2003**, *42*, 2350-2365
- S.H. Yu, H. Cölfen, *J. Mater. Chem.* 2004 in press